



# POLITECNICO MILANO 1863

Homework nr.1 Vibration Analysis and Vibroacoustics 22/23

Riccardo Iaccarino, Rocco Scarano, Enrico Dalla Mora

June 27, 2023

## Contents

|   |          |
|---|----------|
| <b>1 Equations of Motion</b>  | <b>2</b> |
| 1.1 Sign conventions . . . . .  | 2        |
| 1.2 Kinematic analysis . . . . .  | 2        |
| 1.3 Choice of the independent variable . . . . .  | 2        |
| 1.4 Equation of motion of the system for small vibrations around its equilibrium position . . . . . | 2        |
| 1.5 Natural frequency of the system . . . . .   | 4        |
| 1.6 Damping frequency and adimensional damping ratio . . . . .                                      | 4        |
| <b>2 Free Motion</b>  | <b>5</b> |
| 2.1 Resolution of the free response . . . . .   | 5        |
| 2.2 Analysis of a varying damping ratio . . . . .   | 5        |
| <b>3 Forced Motion</b>  | <b>6</b> |
| 3.1 Frequency Response Function $H(\Omega)$ . . . . .   | 6        |
| 3.2 Complete time response to an harmonic torque . . . . .  | 7        |
| 3.3 Insights on different kind of applied torques . . . . .   | 8        |
| <b>4 Response to a multi-harmonic torque</b>  | <b>9</b> |
| 4.1 Time histories . . . . .  | 9        |
| 4.2 Spectra . . . . .   | 10       |

# 1 Equations of Motion

As for every problem of this kind, we first need to set some basic tools that will be useful for its resolution.

## 1.1 Sign conventions

We will consider as positive the elongation of both dampers and springs. The positive sign of the  $x$ ,  $y$  and  $\theta$  will respect the ones in Fig.(1).

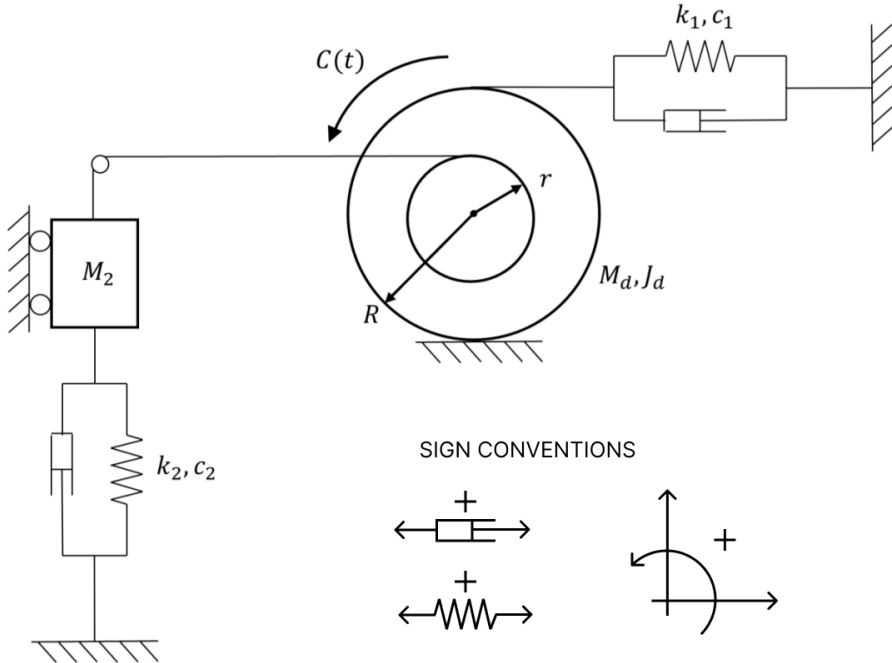


Figure 1: Scheme of the system and sign conventions adopted.

## 1.2 Kinematic analysis

In this section the number of **degrees of freedom** (DOFs) of the system will be analyzed. First of all we have to consider the number of bodies involved (2) that translates in a total of  $3 \cdot k_b = 6$  possible DOFs. From these, we have to subtract  $k_c$ , i.e. the DOFs that have been "locked" by the constraints:

- 2 coming from the point of contact of the disk  $M_d$  with the ground (condition of rolling without slipping);
- 2 related to the slider connected to the mass  $M_2$ , that allows only vertical motion;
- 1 for the inextensible string that connects the two bodies.

Finally, we can compute the total number of DOFs:  $3 \cdot k_b - k_c = 6 - 5 = 1$ .

## 1.3 Choice of the independent variable

As the independent variable of this problem we chose  $\theta$ , the **rotation in counterclockwise direction** of the disk (taken from its static equilibrium position).

## 1.4 Equation of motion of the system for small vibrations around its equilibrium position

The equation of motion can be derived using many different methods, in this case the **Langrangian approach** will be chosen. It consists in solving the following equation (that has been written taking

into account the independent variable previously chosen):

$$\frac{d}{dt} \left( \frac{\partial E_k}{\partial \dot{\theta}} \right) - \frac{\partial E_k}{\partial \theta} + \frac{\partial D}{\partial \dot{\theta}} + \frac{\partial V}{\partial \theta} = \frac{\delta W}{\delta \theta} \quad (1)$$

Hence the first step will be to compute each different form of energy appearing in the formula, that will be later expressed as a function of the independent variable  $\theta$ . In order to understand the forces acting on our system we will analyze the free body diagrams of the two bodies.

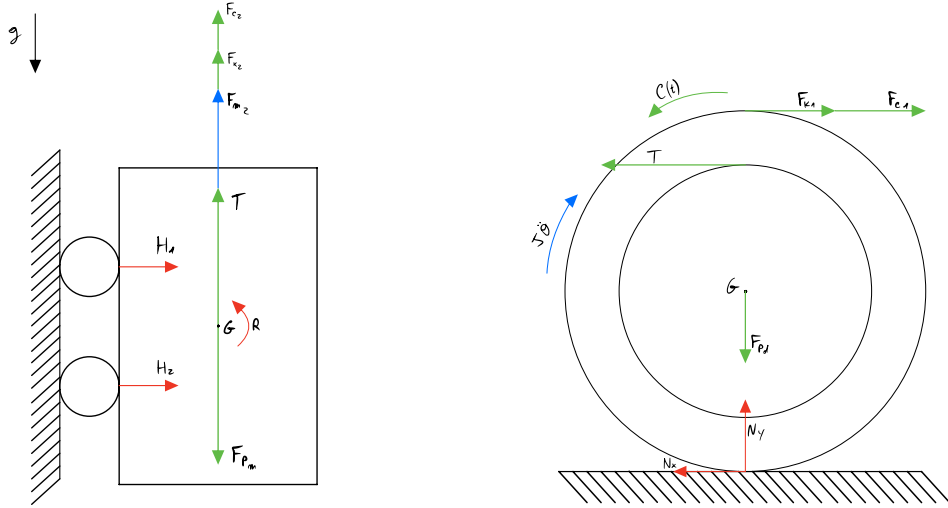


Figure 2: Free body diagrams of the two masses.

We obtain:

- **Kinetic Energy** (roto-translation of the disk and vertical translation of the other mass):

$$E_k = E_{k_1} + E_{k_2} = \frac{1}{2} M_d v_d^2 + \frac{1}{2} J_d \omega_d^2 + \frac{1}{2} M_2 v_2^2 \quad (2)$$

- **Potential Energy** (only elastic contributes, given by the springs):

$$V = V_{el} + V_g = V_1 + V_2 + V_g = \frac{1}{2} K_1 \Delta l_1^2 + \frac{1}{2} K_2 \Delta l_2^2 + M_2 g h_2 \quad (3)$$

- **Dissipative Function** (effect of the presence of the dampers):

$$D = D_1 + D_2 = \frac{1}{2} C_1 \Delta l_1^2 + \frac{1}{2} C_2 \Delta l_2^2 \quad (4)$$

- **Virtual Work** (refers to the applied torque):

$$\delta W = C(t) \delta \theta. \quad (5)$$

Now we need to compute the kinematic relations between our independent variable and the other ones present in the forms of energy:

$$\begin{aligned} \Delta l_1 &= 2R\theta & \Delta l_2 &= -(R+r)\theta \\ \dot{\Delta l}_1 &= 2R\dot{\theta} & \dot{\Delta l}_2 &= -(R+r)\dot{\theta} \\ v_d &= -R\dot{\theta} & v_2 &= -(R+r)\dot{\theta} \\ \omega_d &= \dot{\theta} & h_2 &= -(R+r)\theta \end{aligned}$$

We can exploit these relations and substitute them in the forms of energy:

$$E_k = \frac{1}{2} \dot{\theta}^2 \left( M_d R^2 + J_d + M_2 (R+r)^2 \right) = \frac{1}{2} J^* \dot{\theta}^2 \quad (6)$$

$$V = \frac{1}{2}\theta^2 \left( K_1 4R^2 + K_2(R+r)^2 \right) - M_2 g(R+r)\theta = \frac{1}{2}K_t^* \theta^2 - M_2 g(R+r)\theta \quad (7)$$

$$D = \frac{1}{2}\dot{\theta}^2 \left( C_1 4R^2 + C_2(R+r)^2 \right) = \frac{1}{2}C_t^* \dot{\theta}^2 \quad (8)$$

$$\delta W = C(t) \delta\theta \quad (9)$$

Where:

- $J^* = M_d R^2 + J_d + M_2(R+r)^2$  is the equivalent **mass moment of inertia**;
- $C_t^* = C_1 4R^2 + C_2(R+r)^2$  is the equivalent **torsional damping**;
- $K_t^* = K_1 4R^2 + K_2(R+r)^2$  is the equivalent **torsional stiffness**.

Finally, we can derive these expressions according to (1) in order to get the general equation of motion of a 1-DOF system:

$$J^* \ddot{\theta} + C_t^* \dot{\theta} + K_t^* \theta - M_2 g(R+r)\theta = C(t) \quad (10)$$

Since we are dealing with the system in its equilibrium position  $\theta_e$ , we can impose:

$$\frac{\partial V}{\partial \theta} \Big|_{\theta=\theta_e} = 0 \quad \Rightarrow \quad K_t^* \theta - M_2 g(R+r) = 0 \quad \Rightarrow \quad \theta_e = \frac{M_2 g(R+r)}{K_t^*} \quad (11)$$

Therefore we can substitute our independent variable with a new one:  $\bar{\theta} = \theta - \theta_e$ . Computing the derivatives of  $\bar{\theta}$  and applying them to (10) we obtain:

$$J^* \ddot{\bar{\theta}} + C_t^* \dot{\bar{\theta}} + K_t^* \bar{\theta} = C(t) \quad (12)$$

to which we will refer from now on, using  $\theta$  for simplicity of notation.

## 1.5 Natural frequency of the system

In order to compute the natural frequency of our system, we must exclude the effect of the damping and of any external forces applied. The resulting problem is also called **free response of the undamped system** and refers to the following equation:

$$J^* \ddot{\theta} + K_t^* \theta = 0 \quad (13)$$

This kind of differential equation presents solutions in the form  $\theta(t) = \theta_0 e^{\lambda t}$ , hence we can easily move from (13) to its characteristic equation (in order to find the non-trivial solution):

$$J^* \lambda^2 + K_t^* = 0 \quad (14)$$

From the previous equation we are able to compute the two **complex conjugates eigenvalues**  $\lambda_{1,2} = \pm i\omega_0$ , from which we can get the natural frequency of the system:

$$\omega_0 = \sqrt{\frac{K_t^*}{J^*}} = 7.6715 \text{ rad/s} \quad (15)$$

## 1.6 Damping frequency and adimensional damping ratio

At this point we can move to the **damped case** and once again we will consider the free motion of the system, that has the following characteristic equation:

$$J^* \lambda^2 + C_t^* \lambda + K_t^* = 0 \quad (16)$$

In this case the eigenvalues (still complex conjugates) assume the form:

$$\lambda_{1,2} = -\alpha \pm i\omega_d = -\alpha \pm i\sqrt{\omega_0^2 - \alpha^2} \quad (17)$$

In terms of parameters of the system, this expression (which comes from the resolution of the characteristic equation) can be rewritten as:

$$\lambda_{1,2} = -\frac{C_t^*}{2J^*} \pm i\sqrt{\frac{K_t^*}{J^*} - \left(\frac{C_t^*}{2J^*}\right)^2} \quad (18)$$

Where it becomes clear that  $\alpha = \frac{C_t^*}{2J^*}$ . Moreover, computing the damping frequency becomes a trivial operation:

$$\omega_d = \sqrt{\omega_0^2 - \alpha^2} = 7.6608 \text{ rad/s} \quad (19)$$

In order to obtain the adimensional damping ratio, we can compute the **critical damping** which comes from imposing a null determinant in (17):  $C_{cr} = 2J^*\omega_0$ . This will be helpful in the *viscous damping factor's formula*:

$$h = \frac{C_t^*}{C_{cr}} = \frac{\alpha}{\omega_0} = 5.3 \times 10^{-2} \quad (20)$$

## 2 Free Motion

### 2.1 Resolution of the free response

The free motion of a generic system can be written in three different forms, involving either complex exponentials or sinusoids. We chose to represent it via the second form, which includes both a cosine and a sine contribution:

$$\theta(t) = e^{-\alpha t} [A \cos(\omega_d t) + B \sin(\omega_d t)] \quad (21)$$

where  $\alpha$  as the argument of a negative exponential highlights the effect of damping on the outcome, whereas  $A$  and  $B$  have to be computed starting from the arbitrary chosen **initial conditions**:

$$\begin{cases} \theta(t=0) = 1 \text{ rad} = \theta_0 \\ \dot{\theta}(t=0) = 12 \text{ rad/s} = \dot{\theta}_0 \end{cases} \quad (22)$$

Merging the information from (21) and (22), we can easily obtain our two constants as follows:

$$\begin{cases} A = \theta_0 = 1 \\ B = \frac{\dot{\theta}_0 + \alpha\theta_0}{\omega_d} = 1.6195 \end{cases} \quad (23)$$

It follows that the free motion of our system is fully described by:

$$\theta(t) = e^{-0.407t} [\cos(7.66t) + 1.62 \sin(7.66t)]$$

taking into account that  $\alpha$  and  $\omega_d$  (and so  $B$  as well) depend on  $h$ , as we will discuss in the following paragraph.

### 2.2 Analysis of a varying damping ratio

The three cases proposed by the problem let us study three different types of system, referring to the plots of Fig.(3):

- *slightly damped* ( $h \ll 1$ ): without modifying the parameters of our system, the resulting adimensional damping ratio is  $h = 5.3 \times 10^{-2}$  and as we can see in the **first plot** the system is able to complete many oscillation before experiencing a substantial attenuation;
- *underdamped* ( $h < 1$ ): with a damping ratio 4 times larger the effect of the dampers becomes even more evident; indeed the distinguishable oscillations performed by our system reduce to just 2 or 3 (**second plot**);
- *overdamped* ( $h > 1$ ): finally, with the highest damping factor the system cannot even complete the first iteration of its sinusoidal motion and from the **last plot** we can observe how it takes 1s ca. to stop definitively.

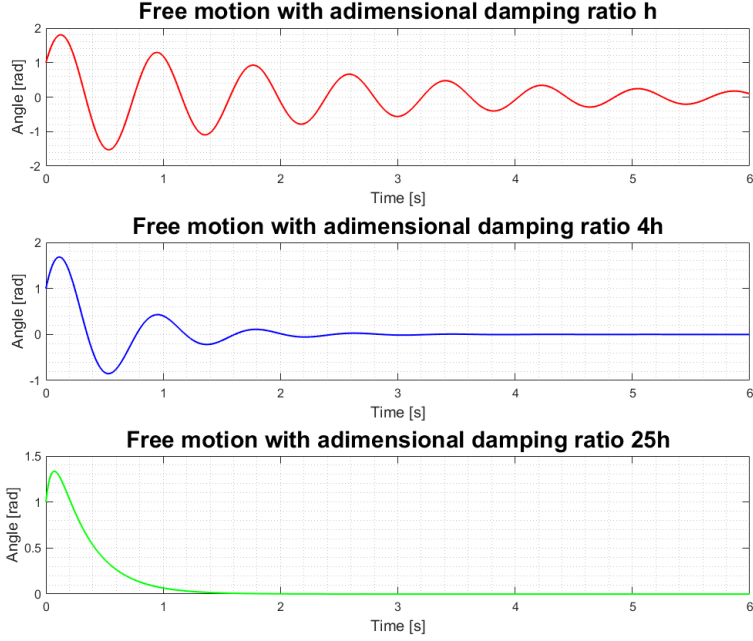


Figure 3: Time response of the system at different values of  $h$ .

### 3 Forced Motion

#### 3.1 Frequency Response Function $H(\Omega)$

For a generic harmonic force applied, the corresponding equation of motion is a second order, non homogeneous, differential equation as already presented in (12). Moreover, we can rewrite the torque as  $C(t) = C_0 \cos(\Omega t + \beta)$  in order to get a solution in the same form:

$$\theta(t) = \theta_0 \cos(\Omega t + \beta + \phi) \quad (24)$$

Unfortunately, this kind of problem turns out to be particularly challenging, so we will pass to the complex (and more general) problem that focuses on  $\tilde{C}(t) = C_0 e^{\Omega t + \beta}$  and  $\tilde{\theta}(t) = \tilde{\theta}_0 e^{\Omega t + \beta + \phi}$ . In fact, after deriving our independent variable, we can get the expression:

$$(-J^* \Omega^2 + C_t^* \Omega + K_t^*) \tilde{\theta}_0 = C_0 \quad (25)$$

At this point getting the **Frequency Response Function** becomes a trivial operation:

$$H(\Omega) = \frac{\tilde{\theta}_0}{C_0} = \frac{1}{-J^* \Omega^2 + C_t^* \Omega + K_t^*} \quad (26)$$

In order to observe the behaviours in frequency w.r.t. the three values of the damping ratio, we must ensure that it appears in the formula of the **FRF**. After some substitutions we can obtain the more suitable form:

$$H(\Omega) = \frac{\frac{1}{K}}{\left(1 - \frac{\Omega^2}{\omega_0^2}\right) + i \left(2h \frac{\Omega}{\omega_0}\right)} \quad (27)$$

To plot the magnitude and phase of (27) we rely on the MATLAB functions `angle()` and `abs()`, but we can also separate them analytically:

$$|H(\Omega)| = \frac{\frac{1}{K}}{\sqrt{\left(1 - \frac{\Omega^2}{\omega_0^2}\right)^2 + \left(2h \frac{\Omega}{\omega_0}\right)^2}} \quad \angle H(\Omega) = \arctan \left( \frac{-2h \frac{\Omega}{\omega_0}}{1 - \frac{\Omega^2}{\omega_0^2}} \right) \quad (28)$$

As we can see from Fig.(4), all the plots have a similar behaviour which can be analyzed through a subdivision in three zones (which counts also as a general study for any 1-DOF system):

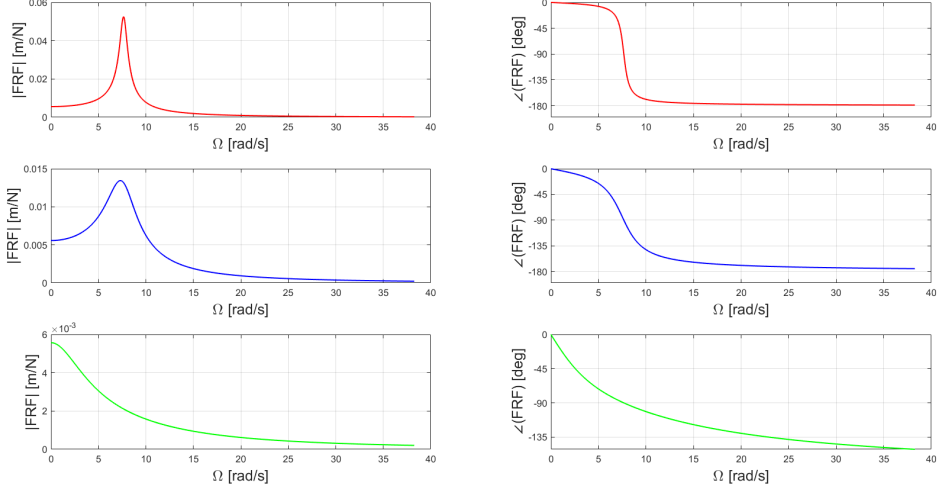


Figure 4: Frequency Response Functions for different values of the damping ratio ( $h$ ,  $4h$ ,  $25h$ ).

- the region prior to the peak of the FRF shows that the output of the system (rotation  $\theta$  in our case) will be in phase with the force applied. Furthermore, the amplitude response happens to be comparable to the static case, which is the reason why it is called **quasi-static zone**;
- towards the natural frequency of the system we can find the **resonance zone**, where the gain assumes the form of a spike and the phase lies around  $\frac{\pi}{2}$ ;
- finally there is the **seismographic zone**, which is characterized by a descending amplitude response (towards a null gain) and a phase that is headed for  $\pi$ .

### 3.2 Complete time response to an harmonic torque

The response of a linear system to an harmonic force (torque) comes from the resolution of (12) and consists in the combination of its general and particular solutions  $\theta(t) = \theta_g(t) + \theta_p(t)$ . We have already found the first term with the analysis of the free vibration (21), hence we now need to extract the second one and we can easily do that thanks to a property of linear systems. Indeed, when dealing with harmonic forces (torques) applied to one of the bodies, we know that the output of our system (the independent variable) can be expressed in the same form of the input. In particular the sinusoid will be modified in amplitude and phase according to the FRF, but it will maintain the same frequency:

$$C(t) = A \cos(2\pi f_1 t + \varphi) \quad \theta_p(t) = |H(\Omega)| C_0 \cos(2\pi f_1 t + \beta + \angle H(\Omega)) \quad (29)$$

The complete solution is the sum of the two components and it is characterized by a transient (related to the general solution) that happens at damping frequency  $\omega_d$ :

$$\theta(t) = e^{-\alpha t} [A \cos(\omega_d t) + B \sin(\omega_d t)] + |H(\Omega)| C_0 \cos(2\pi f_1 t + \beta + \angle H(\Omega)) \quad (30)$$

In order to better observe this phenomenon we chose to plot the time response of the system with slightly different initial conditions:

$$\begin{cases} \theta_0 = 0.1 \text{ rad} \\ \dot{\theta}_0 = 0.2 \text{ rad/s} \end{cases} \quad (31)$$

From Fig.(5) it is appreciable to notice the various feature of the forced motion: its two components at different frequencies, one everlasting and one exponentially decreasing; the total response that approximates the free response in the first stages to then drift towards the shape of the forced one.

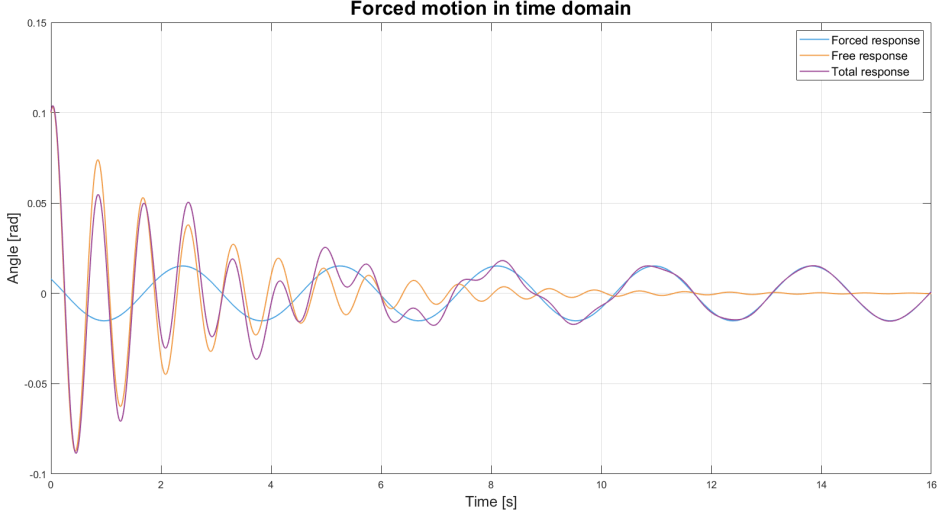


Figure 5: Total response of the system and distinction of general and particular solution.

### 3.3 Insights on different kind of applied torques

In this paragraph we will discuss three cases of interest about the dynamics of our system.

- dynamically applied torque: we can compute the amplitude of the FRF for the two requested cases  $f_1 = 0.35 \text{ Hz}$  and  $f_2 = 10 \text{ Hz}$  by just substituting them in the first equation of (28):

$$|H(\Omega = 2\pi f_1)| = 6.1 \times 10^{-3} \text{ rad} \quad |H(\Omega = 2\pi f_2)| = 2.33 \times 10^{-4} \text{ rad}$$

In order to get the amplitude of the time response at steady-state we have to multiply these values by the amplitude of the force applied ( $C_0 = 2.5 \text{ N}$ ), as can be seen in the amplitude term of  $\theta_p(t)$  (29).

- statically applied torque: "statical" just implies that  $\Omega = 0$ , so the result can be obtain as in the previous point, where:

$$|H(\Omega = 0)| = 5.6 \times 10^{-3} \text{ rad}$$

- comparison with the steady-state response: as we can see from Fig.(6) and Fig.(7), the trend of the torque compared to the steady-state response appears very similar, regardless of the frequency of analysis. What changes from  $f_1$  to  $f_2$  is the relative phase that can be observed by looking at the two compared graphs, which happens to be more significant in the second case.

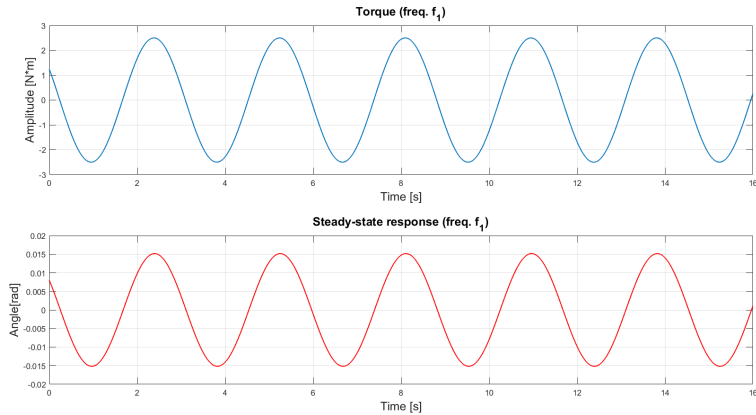


Figure 6: Comparison of the applied torque (with frequency  $f_1$ ) with the steady-state response.

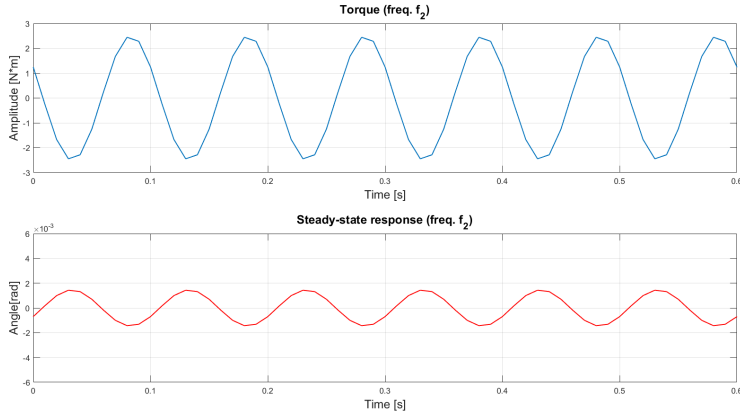


Figure 7: Comparison of the applied torque (with frequency  $f_2$ ) with the steady-state response.

## 4 Response to a multi-harmonic torque

The last section of the study is focused on the dynamics of our system when excited with a torque which is the superposition of three sinusoidal contributions:

$$C(t) = \sum_{k=1}^3 B_k \cos(2\pi f_k t + \beta_k) \quad (32)$$

whose values are listed in the following table:

| $k$       | 1       | 2       | 3       |
|-----------|---------|---------|---------|
| $B_k$     | 1.2     | 0.5     | 5       |
| $f_k$     | 0.35    | 2.5     | 10      |
| $\beta_k$ | $\pi/4$ | $\pi/5$ | $\pi/6$ |

Table 1: Coefficients of the torque.

### 4.1 Time histories

In order to evaluate the steady-state response of the system to torque in (32), we can once again exploit a property of linear systems. Indeed it is possible to compute the response of each harmonic component separately, and then sum up the three contributions obtained. Similarly to (29), we will get:

$$\theta_p(t) = \sum_{k=1}^3 |H(2\pi f_k)| B_k \cos(2\pi f_k t + \beta_k + \angle H(2\pi f_k)) \quad (33)$$

From Fig.(8) we can clearly see how the components at higher frequency have been suppressed by the system, making them become some kind of a ripple over the lowest frequency harmonic of the torque, which is barely distinguishable in the first plot.

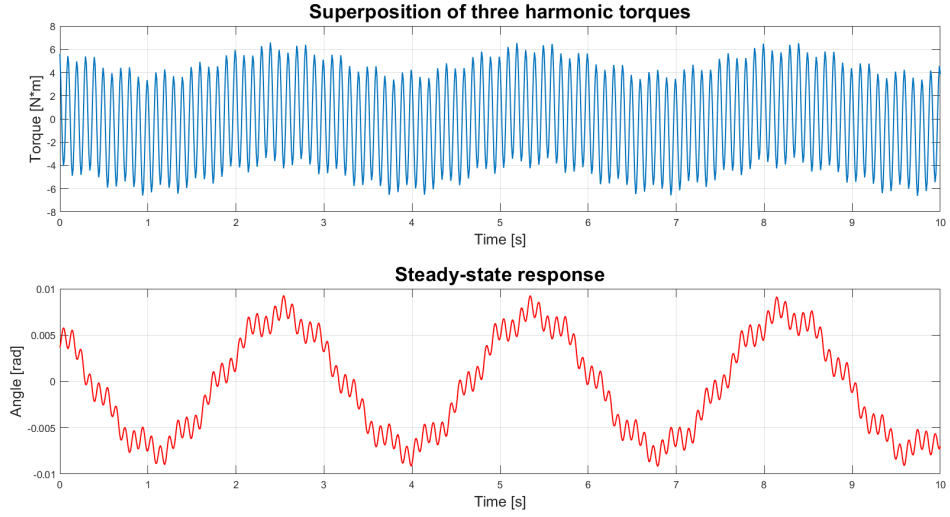


Figure 8: Time histories of applied torque and relative steady-state response.

## 4.2 Spectra

Obtaining the spectrum of the applied torque is a trivial operation because of its structure (linear combination of sinusoids), whereas for the steady-state we need one extra step. In order to get the amplitude response it is possible to multiply the torque's and FRF's spectra Fig.(4), while for the phase one we need to add them:

$$|\theta_{p_k}(\Omega)| = B_k |H(\Omega)|$$

$$\angle \theta_{p_k}(\Omega) = \beta_k + \angle H(\Omega)$$

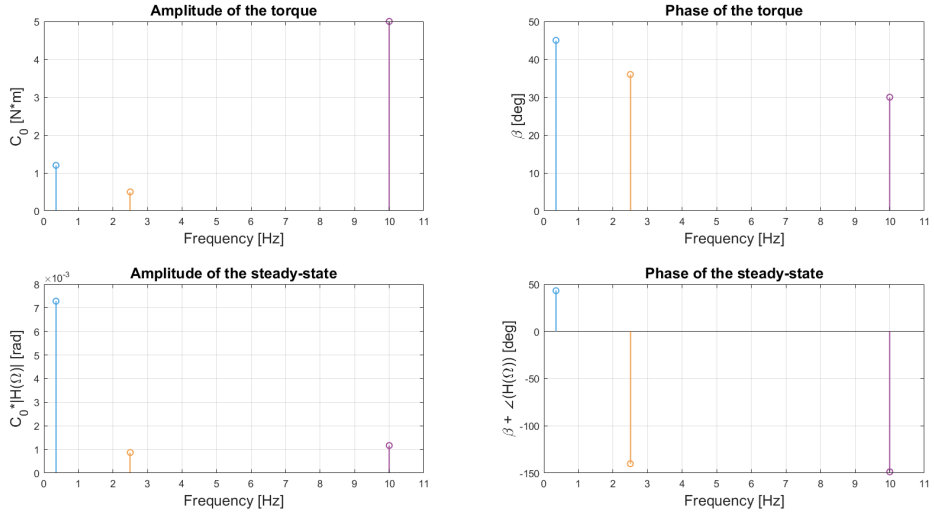


Figure 9: Spectra of the amplitude and phase of the torque and steady-state response of the system.

From both domains it is clear that the system acts as a low pass filter.



# POLITECNICO MILANO 1863

Homework nr.2 Vibration Analysis and Vibroacoustics 22/23

Riccardo Iaccarino, Rocco Scarano, Enrico Dalla Mora

June 27, 2023

## Contents

|   |           |
|---|-----------|
| <b>1 Equations of Motion</b>                                      | <b>2</b>  |
| 1.1 Sign conventions . . . . .                                    | 2         |
| 1.2 Kinematic analysis . . . . .                                  | 2         |
| 1.3 Choice of the independent variables . . . . .                 | 2         |
| 1.4 Equation of motion and system matrices . . . . .              | 3         |
| 1.5 Eigenfrequencies and eigenvectors . . . . .                   | 5         |
| 1.6 Rayleigh Damping . . . . .                                    | 7         |
| <b>2 Free motion of the system</b>                                | <b>8</b>  |
| 2.1 Given initial conditions . . . . .                            | 8         |
| 2.2 Particular initial conditions . . . . .                       | 9         |
| <b>3 Forced motion of the system</b>                              | <b>10</b> |
| 3.1 Frequency response matrix . . . . .                           | 10        |
| 3.2 Co-located FRF in A . . . . .                                 | 12        |
| 3.3 Co-located FRF for $\theta_2$ . . . . .                       | 12        |
| 3.4 Complete time response . . . . .                              | 13        |
| 3.5 Steady-state response of a periodic triangular wave . . . . . | 15        |
| <b>4 Modal approach</b>   | <b>16</b> |
| 4.1 Equations of motion in modal coordinates . . . . .            | 16        |
| 4.2 Co-located FRF Reconstruction of point A . . . . .            | 17        |
| 4.3 Co-located FRF Reconstruction for $\theta_2$ . . . . .        | 19        |
| 4.4 Steady state amplitude of response . . . . .                  | 19        |
| <b>5 Optional</b>   | <b>21</b> |
| 5.1 Graphical representation of the mode shapes . . . . .         | 21        |
| 5.2 FRF representation using different diagrams . . . . .         | 22        |

# 1 Equations of Motion

As for every problem of this kind, we first need to set some basic tools that will be useful for its resolution.

## 1.1 Sign conventions

We will consider as positive the elongation of both dampers and springs. The positive sign of the  $x$ ,  $y$  and  $\theta$  will respect the ones in Fig.(1).

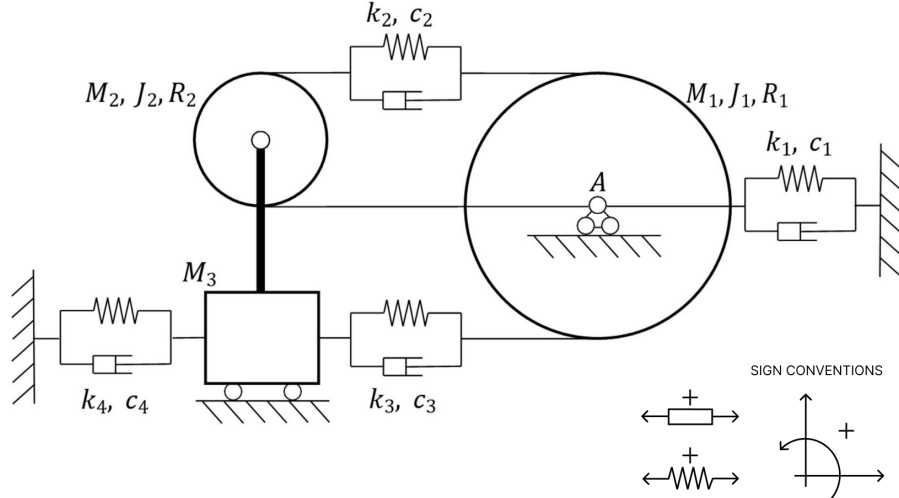


Figure 1: Scheme of the system and sign conventions adopted.

## 1.2 Kinematic analysis

In this section the number of **degrees of freedom** (DOFs) of the system will be analyzed. First of all we have to consider the number of bodies involved (3) that translates in a total of  $k_b = 9$  possible DOFs. From these, we have to subtract  $k_c$ , i.e. the DOFs that have been "locked" by the constraints:

- 1 coming from the roller attached to the center of the disk  $M_1$ , which blocks the vertical displacement of the mass;
- 1 for the inextensible string that connects the center of the mass  $M_1$  to the disk  $M_2$ ;
- 2 coming from the hinge in the center of the disk  $M_2$ ;
- 2 for the rollers of the mass  $M_3$  which exclude vertical motion and rotation;

Finally, we can compute the total number of DOFs:  $3 \cdot k_b - k_c = 9 - 6 = 3$

## 1.3 Choice of the independent variables

As we have seen, the system presents 3 DOFs, hence we will need 3 independent variables. To analyze this problem we chose:

- $\theta_1$ , the absolute counter-clockwise **rotation** of the disk  $M_1$  around its center A (taken from its static equilibrium position);
- $\theta_2$ , the absolute counter-clockwise **rotation** of the disk  $M_2$  around its center (taken from its static equilibrium position);
- $x_3$ , the **horizontal motion** of the mass  $M_3$  in the positive  $x$  direction (taken from its static equilibrium position);

From now on, we will work with these variables using the vector:

$$\underline{x} = \begin{Bmatrix} \theta_1 \\ \theta_2 \\ x_3 \end{Bmatrix} \quad (1)$$

## 1.4 Equation of motion and system matrices

The equation of motion can be derived using many different methods, in this case the **Langrangian approach** (in vectorial form) will be chosen. It consists in solving the following equation (that has been written taking into account the vector of independent variables previously chosen):

$$\left\{ \frac{d}{dt} \left( \frac{\partial E_k}{\partial \dot{\underline{x}}} \right) \right\}^T - \left\{ \frac{\partial E_k}{\partial \underline{x}} \right\}^T + \left\{ \frac{\partial D}{\partial \dot{\underline{x}}} \right\}^T + \left\{ \frac{\partial V}{\partial \underline{x}} \right\}^T = \underline{Q}_x \quad (2)$$

Although the first step should be to compute each different form of energy appearing in the formula, we prefer to first define some vectors that will simplify our operations. First of all we have to take into account every variable that characterize the motion of the system and to do so we can employ just two vectors and their derivatives:

$$\underline{y} = \begin{Bmatrix} x_1 \\ \theta_1 \\ x_2 \\ \theta_2 \\ x_3 \end{Bmatrix} \quad \dot{\underline{y}} = \begin{Bmatrix} \dot{x}_1 \\ \dot{\theta}_1 \\ \dot{x}_2 \\ \dot{\theta}_2 \\ \dot{x}_3 \end{Bmatrix} = \begin{Bmatrix} v_1 \\ \omega_1 \\ v_2 \\ \omega_2 \\ v_3 \end{Bmatrix} \quad \underline{\Delta l} = \begin{Bmatrix} \Delta l_1 \\ \Delta l_2 \\ \Delta l_3 \\ \Delta l_4 \end{Bmatrix} \quad \dot{\underline{\Delta l}} = \begin{Bmatrix} \dot{\Delta l}_1 \\ \dot{\Delta l}_2 \\ \dot{\Delta l}_3 \\ \dot{\Delta l}_4 \end{Bmatrix} \quad (3)$$

where the terms  $x_i$  and  $\theta_i$  are respectively the i-th body's vertical motion and absolute rotation and the terms  $\Delta l_i$  are the absolute elongations of springs and dampers. Now we can go on and calculate the forms of energy and consequently the system matrices:

- **Kinetic Energy:**

$$E_k = \frac{1}{2} M_1 v_1^2 + \frac{1}{2} J_1 \omega_1^2 + \frac{1}{2} M_2 v_2^2 + \frac{1}{2} J_2 \omega_2^2 + \frac{1}{2} M_3 v_3^2 \quad (4)$$

Since we want to write each form of energy with matrices and vectors, for the kinetic energy we will refer to  $E_k = \frac{1}{2} \dot{\underline{y}}^T [M_{ph}] \dot{\underline{y}}$ . This formula let us write the matrix of the coefficients of the variables:

$$[M_{ph}] = \begin{bmatrix} M_1 & 0 & 0 & 0 & 0 \\ 0 & J_1 & 0 & 0 & 0 \\ 0 & 0 & M_2 & 0 & 0 \\ 0 & 0 & 0 & J_2 & 0 \\ 0 & 0 & 0 & 0 & M_3 \end{bmatrix} \quad (5)$$

Moreover, we can rewrite  $\dot{\underline{y}}$  highlighting its dependence on  $\dot{\underline{x}}$ , thanks to the **Jacobians**. We can use the relation:

$$\dot{\underline{y}} = \left( \frac{\partial \underline{y}}{\partial \dot{\underline{x}}} \right) \dot{\underline{x}} = [\Lambda_m] \dot{\underline{x}} \quad (6)$$

Where  $[\Lambda_m]$  is indeed the **Jacobian matrix** which contains the partial derivatives of each variable of  $\dot{\underline{y}}$  w.r.t. the independent variables of  $\dot{\underline{x}}$ :

|                  | $\dot{\theta}_1$ | $\dot{\theta}_2$ | $\dot{x}_3$ |
|------------------|------------------|------------------|-------------|
| $\dot{x}_1$      | 0                | $R_2$            | 1           |
| $\dot{\theta}_1$ | 1                | 0                | 0           |
| $\dot{x}_2$      | 0                | 0                | 1           |
| $\dot{\theta}_2$ | 0                | 1                | 0           |
| $\dot{x}_3$      | 0                | 0                | 1           |

$$\Rightarrow [\Lambda_m] = \begin{bmatrix} 0 & R_2 & 1 \\ 1 & 0 & 0 \\ 0 & 0 & 1 \\ 0 & 1 & 0 \\ 0 & 0 & 1 \end{bmatrix} \quad (7)$$

At this point we can put all together to get the final expression of the kinetic energy:

$$E_k = \frac{1}{2} \dot{\underline{y}}^T [M_{ph}] \dot{\underline{y}} = \frac{1}{2} \dot{\underline{x}}^T [\Lambda_m]^T [M_{ph}] [\Lambda_m] \dot{\underline{x}} = \frac{1}{2} \dot{\underline{x}}^T [M^*] \dot{\underline{x}} \quad (8)$$

with  $[M^*]$  being the **mass matrix** of our system, that is easily computed as:

$$[M^*] = [\Lambda_m]^T [M_{ph}] [\Lambda_m] = \begin{bmatrix} J_1 & 0 & 0 \\ 0 & M_1 R_2^2 + J_2 & M_1 R_2 \\ 0 & M_1 R_2 & M_1 + M_2 + M_3 \end{bmatrix} \quad (9)$$

- **Potential Energy:**

$$V = \frac{1}{2} K_1 \Delta l_1^2 + \frac{1}{2} K_2 \Delta l_2^2 + \frac{1}{2} K_3 \Delta l_3^2 + \frac{1}{2} K_4 \Delta l_4^2 \quad (10)$$

Since we are considering the system in its equilibrium position, for the potential energy we will refer to  $V = \frac{1}{2} \underline{\Delta l}^T [K_{ph}] \underline{\Delta l}$ , neglecting the term related to the gravitational potential energy. This formula let us write the matrix of the coefficients of the variables:

$$[K_{ph}] = \begin{bmatrix} K_1 & 0 & 0 & 0 \\ 0 & K_2 & 0 & 0 \\ 0 & 0 & K_3 & 0 \\ 0 & 0 & 0 & K_4 \end{bmatrix} \quad (11)$$

As for the previous form of energy, we exploit the relation:

$$\underline{\Delta l} = \left( \frac{\partial \underline{\Delta l}}{\partial \underline{x}} \right) \underline{x} = [\Lambda_k] \underline{x} \quad (12)$$

Where  $[\Lambda_k]$  is indeed the **Jacobian matrix** which contains the partial derivatives of each variable of  $\underline{\Delta l}$  w.r.t. the independent variables of  $\underline{x}$ :

|              | $\theta_1$ | $\theta_2$ | $x_3$ |
|--------------|------------|------------|-------|
| $\Delta l_1$ | 0          | $-R_2$     | -1    |
| $\Delta l_2$ | $-R_1$     | $2R_2$     | 0     |
| $\Delta l_3$ | $R_1$      | $R_2$      | 0     |
| $\Delta l_4$ | 0          | 0          | 1     |

$$\Rightarrow [\Lambda_k] = \begin{bmatrix} 0 & -R_2 & -1 \\ -R_1 & 2R_2 & 0 \\ R_1 & R_2 & 0 \\ 0 & 0 & 1 \end{bmatrix} \quad (13)$$

At this point we can put all together to get the final expression of the potential energy:

$$V = \frac{1}{2} \underline{\Delta l}^T [K_{ph}] \underline{\Delta l} = \frac{1}{2} \underline{x}^T [\Lambda_k]^T [K_{ph}] [\Lambda_k] \underline{x} = \frac{1}{2} \underline{x}^T [K^*] \underline{x} \quad (14)$$

with  $[K^*]$  being the **stiffness matrix** of our system which can be computed as:

$$[K^*] = [\Lambda_k]^T [K_{ph}] [\Lambda_k] = \begin{bmatrix} R_1^2 K_2 + R_1^2 K_3 & R_1 R_2 K_3 - 2R_1 R_2 K_2 & 0 \\ R_1 R_2 K_3 - 2R_1 R_2 K_2 & R_2^2 K_1 + 4R_2^2 K_2 + R_2^2 K_3 & R_2 K_1 \\ 0 & R_2 K_1 & K_1 + K_4 \end{bmatrix} \quad (15)$$

- **Dissipative Function:**

$$D = \frac{1}{2} C_1 \dot{\Delta l}_1^2 + \frac{1}{2} C_2 \dot{\Delta l}_2^2 + \frac{1}{2} C_3 \dot{\Delta l}_3^2 \quad (16)$$

Once again we want to obtain a function in the form  $D = \frac{1}{2} \dot{\underline{\Delta l}}^T [C_{ph}] \dot{\underline{\Delta l}}$  and we can easily find the diagonal damping matrix:

$$[C_{ph}] = \begin{bmatrix} C_1 & 0 & 0 & 0 \\ 0 & C_2 & 0 & 0 \\ 0 & 0 & C_3 & 0 \\ 0 & 0 & 0 & C_4 \end{bmatrix} \quad (17)$$

The next steps will be dual to the procedure used for the potential energy, in fact we exploit the relation:

$$\dot{\underline{\Delta l}} = \left( \frac{\partial \dot{\underline{\Delta l}}}{\partial \dot{\underline{x}}} \right) \dot{\underline{x}} = [\Lambda_c] \dot{\underline{x}} \quad (18)$$

Where  $[\Lambda_c]$  is the **Jacobian matrix** and presents the very same coefficients of  $[\Lambda_k]$ :

$$[\Lambda_c] = \begin{bmatrix} 0 & -R_2 & -1 \\ -R_1 & 2R_2 & 0 \\ R_1 & R_2 & 0 \\ 0 & 0 & 1 \end{bmatrix} = [\Lambda_k] \quad (19)$$

At this point we can put all together to get the final expression of the dissipative energy:

$$D = \frac{1}{2} \underline{\Delta l}^T [C_{ph}] \underline{\Delta l} = \frac{1}{2} \dot{x}^T [\Lambda_c]^T [C_{ph}] [\Lambda_c] \dot{x} = \frac{1}{2} \dot{x}^T [C^*] \dot{x} \quad (20)$$

with  $[C^*]$  being the **damping matrix** of our system which is in the same form of  $[K^*]$ , except for the stiffness coefficients that have been replaced by the damping ones:

$$[C^*] = [\Lambda_c]^T [C_{ph}] [\Lambda_c] = \begin{bmatrix} R_1^2 C_2 + R_1^2 C_3 & R_1 R_2 C_3 - 2R_1 R_2 C_2 & 0 \\ R_1 R_2 C_3 - 2R_1 R_2 C_2 & R_2^2 C_1 + 4R_2^2 C_2 + R_2^2 C_3 & R_2 C_1 \\ 0 & R_2 C_1 & C_1 + C_4 \end{bmatrix} \quad (21)$$

- **Lagrangian component:**

$$\underline{Q}_x = \left\{ \frac{\partial W}{\partial \underline{x}} \right\}^T \quad (22)$$

In general we would have that  $\partial W = F(t) \cdot \delta^*$  where the virtual displacement  $\delta^*$  can be written as a function of the independent variables by means of a proper Jacobian matrix  $[\Lambda_\delta]$  as  $\delta^* = [\Lambda_\delta] \delta \underline{x}$ .

In our case, since there's no force applied as we can see from the system's scheme, the infinitesimal virtual work contribution will be null.

Finally, we can rewrite the equation (2) where the four terms are computed as follows, keeping in mind that we found symmetrical matrices (translation does not affect them!):

$$\begin{aligned} \left\{ \frac{d}{dt} \left( \frac{\partial E_k}{\partial \dot{\underline{x}}} \right) \right\}^T &= \left\{ \frac{d}{dt} (\dot{\underline{x}}^T [M^*]) \right\}^T = [M^*] \ddot{\underline{x}} \\ \left\{ \frac{\partial E_k}{\partial \underline{x}} \right\}^T &= 0 \\ \left\{ \frac{\partial D}{\partial \dot{\underline{x}}} \right\}^T &= \{\dot{\underline{x}}^T [C^*]\}^T = [C^*] \dot{\underline{x}} \\ \left\{ \frac{\partial V}{\partial \underline{x}} \right\}^T &= \{\underline{x}^T [K^*]\}^T = [K^*] \underline{x} \end{aligned}$$

Consequently, the Lagrangian equation becomes:

$$[M^*] \ddot{\underline{x}} + [C^*] \dot{\underline{x}} + [K^*] \underline{x} = 0 \quad (23)$$

## 1.5 Eigenfrequencies and eigenvectors

This subsection is related to the problem of the free vibration of the system ( $\underline{Q}_x = 0$ ) and it will be divided into two parts: the **undamped** case and the **damped** one.

- **Undamped system**

The first case considered is when we assume a null damping, condition that reflects on the homonymous matrix  $[C^*] = 0$ . The EOM can be seen as a set of three homogeneous linear differential equations which assume the matricial form:

$$[M^*] \ddot{\underline{x}} + [K^*] \underline{x} = 0 \quad (24)$$

The previous equation has as a general solution  $\underline{x} = \underline{x}_0 e^{\lambda t}$ , that gives us also  $\ddot{\underline{x}} = \lambda^2 \underline{x}_0 e^{\lambda t}$ . Substituting these expressions in (24), we can get to:

$$[\lambda^2 [M^*] + [K^*]] \underline{x}_0 e^{\lambda t} = 0 \quad (25)$$

Solving for the non trivial solution means imposing the **characteristic equation**:

$$\det\left(\left[\lambda^2[M^*] + [K^*]\right]\right) = 0 \quad (26)$$

which is a  $2n$  polynomial in  $\lambda$  (in this case  $n = 3$ ) that returns 6 different solutions  $\lambda_i$ . Equation (25) can therefore be written as an **eigenvalue-eigenvector problem**:

$$\left[\lambda^2[I] + [M^*]^{-1}[K^*]\right]\underline{X} = 0 \quad (27)$$

whose solutions give us the natural frequencies of the system thanks to the relations

$$\lambda_I = \lambda_{1,4} = \pm i\omega_I \quad \lambda_{II} = \lambda_{2,5} = \pm i\omega_{II} \quad \lambda_{III} = \lambda_{3,6} = \pm i\omega_{III} \quad (28)$$

We can now collect the eigenfrequencies in a vector:

$$\underline{\omega} = \begin{Bmatrix} \omega_1 \\ \omega_2 \\ \omega_3 \\ \omega_4 \\ \omega_5 \\ \omega_6 \end{Bmatrix} = \begin{Bmatrix} +\sqrt{\omega^2_I} \\ +\sqrt{\omega^2_{II}} \\ +\sqrt{\omega^2_{III}} \\ -\sqrt{\omega^2_I} \\ -\sqrt{\omega^2_{II}} \\ -\sqrt{\omega^2_{III}} \end{Bmatrix} = \begin{Bmatrix} 9.7840 \text{ rad/s} \\ 14.1841 \text{ rad/s} \\ 21.1479 \text{ rad/s} \\ -9.7840 \text{ rad/s} \\ -14.1841 \text{ rad/s} \\ -21.1479 \text{ rad/s} \end{Bmatrix} \quad (29)$$

from which we can also compute the eigenvectors  $\underline{X}^{(i)}$  that will represent the three different mode shapes. These can be both expressed in the original form (40) or normalized w.r.t. a given independent variable (41) (we chose the common solution, the first one):

$$\underline{X}^{(I)} = \begin{Bmatrix} -0.3637 \text{ rad} \\ -0.9256 \text{ rad} \\ 0.1046 \text{ m} \end{Bmatrix}, \quad \underline{X}^{(II)} = \begin{Bmatrix} -0.7536 \text{ rad} \\ 0.6574 \text{ rad} \\ -0.0013 \text{ m} \end{Bmatrix}, \quad \underline{X}^{(III)} = \begin{Bmatrix} 0.2809 \text{ rad} \\ -0.6565 \text{ rad} \\ 0.7001 \text{ m} \end{Bmatrix} \quad (30)$$

$$\underline{X}^{(I)} = \begin{Bmatrix} 1 \text{ rad} \\ 2.5449 \text{ rad} \\ -0.2877 \text{ m} \end{Bmatrix}, \quad \underline{X}^{(II)} = \begin{Bmatrix} 1 \text{ rad} \\ -0.8724 \text{ rad} \\ 0.0018 \text{ m} \end{Bmatrix}, \quad \underline{X}^{(III)} = \begin{Bmatrix} 1 \text{ rad} \\ -2.3371 \text{ rad} \\ 2.4924 \text{ m} \end{Bmatrix} \quad (31)$$

### • Damped system

In the damped case we now need to consider  $[C^*] \neq 0$ . The equation of motion now becomes of the form:

$$[M^*]\ddot{\underline{x}} + [C^*]\dot{\underline{x}} + [K^*]\underline{x} = \underline{0} \quad (32)$$

To compute the general solution we notice that:

$$\begin{cases} [M^*]\ddot{\underline{x}} + [C^*]\dot{\underline{x}} + [K^*]\underline{x} = \underline{0} \\ [M^*]\dot{\underline{x}} - [M^*]\dot{\underline{x}} = \underline{0} \end{cases} \Leftrightarrow \begin{bmatrix} [M^*] & [0] \\ [0] & [M^*] \end{bmatrix} \begin{Bmatrix} \ddot{\underline{x}} \\ \dot{\underline{x}} \end{Bmatrix} + \begin{bmatrix} [C^*] & [K^*] \\ -[M^*] & [0] \end{bmatrix} \begin{Bmatrix} \dot{\underline{x}} \\ \underline{x} \end{Bmatrix} = \underline{0} \quad (33)$$

The system has been reduced to its state space form, and can be written in function of its so-called "state space matrix":

$$[A]\dot{\underline{z}} + [B]\underline{z} = \underline{0} \quad (34)$$

where:

$$\underline{z} = \begin{Bmatrix} \dot{\underline{x}} \\ \underline{x} \end{Bmatrix}, \quad [A] = \begin{bmatrix} [M^*] & [0] \\ [0] & [M^*] \end{bmatrix}, \quad [B] = \begin{bmatrix} [C^*] & [K^*] \\ -[M^*] & [0] \end{bmatrix} \quad (35)$$

Since  $[M^*]$  is invertible, so is  $[A]$  and therefore the EOM is simply:

$$\dot{\underline{z}} - [\Lambda_z]\underline{z} = \underline{0}, \quad \text{with } [\Lambda_z] = -[A]^{-1}[B] \quad (36)$$

whose solution is of the form  $\underline{z} = \underline{z}_0 e^{\lambda t}$ .

To compute the different eigenvalues  $\lambda_i$  we exclude the trivial solution  $z_0 = 0$  and look for the roots of the determinant of  $\lambda[I]_{6 \times 6} - [\Lambda_z]$ . These solutions happen to be of the form  $\lambda_i = -\alpha_i + i\omega_i$ , where  $\omega_i$  are the same eigenvalues found previously for the undamped system. In particular, we get

$$\underline{\lambda} = \begin{Bmatrix} \lambda_1 \\ \lambda_2 \\ \lambda_3 \\ \lambda_4 \\ \lambda_5 \\ \lambda_6 \end{Bmatrix} = \begin{Bmatrix} \lambda_I \\ \lambda_{II} \\ \lambda_{III} \\ \lambda_I^* \\ \lambda_{II}^* \\ \lambda_{III}^* \end{Bmatrix} = \begin{Bmatrix} -0.1910 + i9.7838 \text{ rad/s} \\ -0.3036 + i14.1792 \text{ rad/s} \\ -0.3850 + i21.1432 \text{ rad/s} \\ -0.1910 - i9.7838 \text{ rad/s} \\ -0.3036 - i14.1792 \text{ rad/s} \\ -0.3850 - i21.1432 \text{ rad/s} \end{Bmatrix} \quad (37)$$

Consequently the natural damping frequencies are:

$$\omega_{d1} = 9.7838 \text{ rad/s} \quad \omega_{d2} = 14.1792 \text{ rad/s} \quad \omega_{d3} = 21.1432 \text{ rad/s} \quad (38)$$

Moreover, solving for the eigenvectors  $\underline{Z}_i$  we would obtain terms related both to velocities and displacements:

$$\underline{z} = \begin{Bmatrix} \dot{x} \\ x \end{Bmatrix} = \begin{Bmatrix} \lambda \underline{X} e^{\lambda t} \\ \underline{X} e^{\lambda t} \end{Bmatrix} = \begin{Bmatrix} \lambda \underline{X} \\ \underline{X} \end{Bmatrix} e^{\lambda t} = \underline{Z} e^{\lambda t} \quad (39)$$

Considering just the displacements the mode shapes can be expressed in original and normalized form as follows:

$$\underline{X}^{(I)} = \begin{Bmatrix} 0.0021 \pm i0.0285 \text{ rad} \\ -0.0041 \mp i0.0666 \text{ rad} \\ 0.0014 \pm i0.0711 \text{ m} \end{Bmatrix}, \quad \underline{X}^{(II)} = \begin{Bmatrix} -0.0011 \mp i0.0530 \text{ rad} \\ 0.0011 \pm i0.0462 \text{ rad} \\ 0.0006 \mp i0.0001 \text{ m} \end{Bmatrix}, \quad \underline{X}^{(III)} = \begin{Bmatrix} -0.0006 \mp i0.0172 \text{ rad} \\ -0.0008 \mp i0.0437 \text{ rad} \\ -0.0000 \pm i0.0049 \text{ m} \end{Bmatrix} \quad (40)$$

$$\underline{X}^{(I)} = \begin{Bmatrix} 1.0000 \pm i0.0000 \text{ rad} \\ -2.3361 \mp i0.0296 \text{ rad} \\ 2.4856 \pm i0.1356 \text{ m} \end{Bmatrix}, \quad \underline{X}^{(II)} = \begin{Bmatrix} 1.0000 \pm i0.0000 \text{ rad} \\ -0.8731 \pm i0.0014 \text{ rad} \\ 0.0020 \pm i0.0106 \text{ m} \end{Bmatrix}, \quad \underline{X}^{(III)} = \begin{Bmatrix} 1.0000 \pm i0.0000 \text{ rad} \\ 2.5433 \pm i0.0499 \text{ rad} \\ -0.2874 \mp i0.0132 \text{ m} \end{Bmatrix} \quad (41)$$

## 1.6 Rayleigh Damping

We now want to evaluate the two constants  $\alpha$  and  $\beta$  that allow to approximate the generalized damping matrix  $[C^*]$  through the Rayleigh proportional damping formula:

$$[C^*] = \alpha[M^*] + \beta[K^*] \quad (42)$$

In order to do so, we first need to evaluate the adimensional damping coefficients of the system as:

$$\xi = \left| \frac{\alpha}{\omega_o} \right| = \left| \frac{\alpha}{\sqrt{\omega_d^2 + \alpha^2}} \right| \quad (43)$$

where:

$$\underline{\alpha} = Re\{\lambda_d\} \quad \underline{\omega_d} = Im\{\lambda_d\} \quad (44)$$

Transposing to a 1-DOF case we can now express  $\xi$  as:

$$\xi = \frac{c}{c_{cr}} \quad (45)$$

and therefore get the relation between  $\xi$  the coefficients  $\alpha$  and  $\beta$ :

$$\frac{c}{c_{cr}} = \frac{\alpha \cdot m}{2m\omega_0} + \frac{\beta \cdot k}{2m\omega_0} = \frac{1}{2} \frac{\alpha}{\omega_0} + \frac{1}{2} \beta \omega_0 \quad (46)$$

Which, for a generic N-DOF system becomes:

$$\xi_j = \frac{1}{2} \left( \frac{\alpha}{\omega_{0j}} + \beta \omega_{0j} \right) \quad \text{for } j = 1, 2, 3 \quad (47)$$

The actual damping coefficients can be calculated by applying the least square method to determine the least square sum of the difference between the calculated damping ratio of each mode and the actual damping ratios. We obtain:

$$\alpha = 0.2946 \quad \beta = 0.0012 \quad (48)$$

Here we report  $[C^*]$  compared to the equivalent  $[C_R^*]$  calculated with the Rayleigh damping:

$$[C^*] = [\Lambda_c]^T [C_{ph}] [\Lambda_c] = \begin{bmatrix} 1.500 & 0 & 0 \\ 0 & 0.8750 & 0.2500 \\ 0 & 0.2500 & 4.5000 \end{bmatrix} \quad (49)$$

$$[C_R^*] = \alpha[M^*] + \beta[K^*] = \begin{bmatrix} 1.5129 & 0.2118 & 0 \\ 0.2118 & 0.9918 & 1.3246 \\ 0 & 1.3246 & 6.9044 \end{bmatrix} \quad (50)$$

Finally the eigenvectors  $\underline{X}^{(i)}$  and the eigenvalues  $\lambda_i$  have to be computed once again with the new value of  $[C_R^*]$ . From now on all the calculations will refer to these values.

## 2 Free motion of the system

In order to calculate the free motion of the system we need to solve a system of equations given by eq. (32), the relation that characterizes Rayleigh's damping and initial conditions. This is also called Cauchy problem and can be written as follows:

$$\begin{cases} [M^*]\ddot{\underline{x}} + [C_R^*]\dot{\underline{x}} + [K^*]\underline{x} = \underline{0} \\ [C_R^*] = \alpha[M^*] + \beta[K^*] \\ \underline{x}(t=0) = \underline{x}_0 \\ \dot{\underline{x}}(t=0) = \dot{\underline{x}}_0 \end{cases} \quad (51)$$

The solution can be computed as:

$$\underline{x}(t) = \sum_{i=1}^6 a_i \underline{X}^{(i)} e^{\lambda_i t} \quad (52)$$

where  $\underline{X}^{(i)}$  and  $\lambda_i$  are respectively the eigenvectors and the eigenvalues previously defined and since they all come in pairs that are complex conjugates, the solution will be real. Finally,  $a_i$  are the constants of integration and can be derived imposing the initial conditions, in particular:

$$\underline{a} = \left[ \frac{\underline{X}}{\lambda \underline{X}} \right]^{-1} \left\{ \begin{array}{l} \underline{x}_0 \\ \dot{\underline{x}}_0 \end{array} \right\} \quad (53)$$

### 2.1 Given initial conditions

We now impose the following set of initial conditions:

$$\underline{x}_0 = \begin{Bmatrix} \pi/12 \text{ rad} \\ -\pi/12 \text{ rad} \\ 0.1 \text{ m} \end{Bmatrix} \quad \dot{\underline{x}}_0 = \begin{Bmatrix} 0.5 \text{ rad/s} \\ 2 \text{ rad/s} \\ 1 \text{ m/s} \end{Bmatrix} \quad (54)$$

thanks to which we can solve the Cauchy problem (51) and plot the three trends of our independent variables. As we can see in Figure (2) the free response of  $x_3$  presents a dominant first-mode contribution while for  $\theta_1$  and  $\theta_2$  the other modes are more prominent.

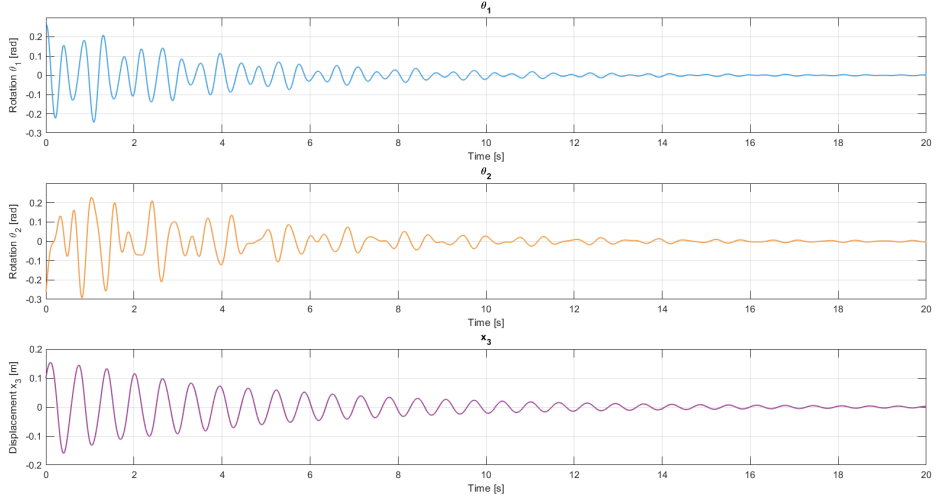


Figure 2: Free motion of the system assuming Rayleigh damping, with given initial conditions.

## 2.2 Particular initial conditions

We now need to choose a particular set of initial conditions in order to get the contribution of only one of the modes. In order to do so we set:

$$\begin{Bmatrix} \underline{x}_0 \\ \underline{\dot{x}}_0 \end{Bmatrix} = \begin{Bmatrix} X^{(1)} \\ 0 \end{Bmatrix} \quad (55)$$

In our case we chose the first mode as the only vibrating one. This last condition is what ensures that one and only one mode is responsible for the free motion of the system. The free response is then calculated as shown in the previous section.

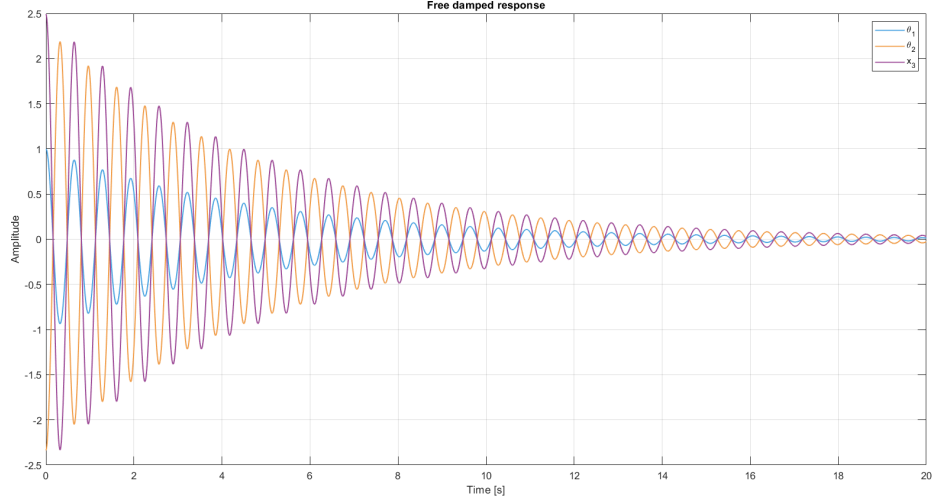


Figure 3: Free motion of the system with initial conditions set so that only the first mode contributes.

### 3 Forced motion of the system

The computation of the forced response of the system follows the same initial steps of the free case: indeed we want to solve once again the Cauchy problem, but this time the first equation will not be homogeneous anymore. This let us introduce the force into the system and in particular it will be written highlighting its dependency from the independent variables  $\underline{x}$ .

$$\begin{cases} [M^*]\ddot{\underline{x}} + [C_R^*]\dot{\underline{x}} + [K^*]\underline{x} = F(t)[\Lambda_\delta]^T \\ [C_R^*] = \alpha[M^*] + \beta[K^*] \\ \underline{x}(t=0) = \underline{x}_0 \\ \dot{\underline{x}}(t=0) = \dot{\underline{x}}_0 \end{cases} \quad (56)$$

The complete time response (or general integral) of the linear system is given by the superposition of two solutions:

$$\underline{x}(t) = \underline{x}_g(t) + \underline{x}_p(t) \quad (57)$$

where  $\underline{x}_g(t)$  is the general solution related to the free homogeneous problem, while  $\underline{x}_p(t)$  is the so called steady state response or particular solution (since it is associated to the external force). The former solution has already been computed and its expression is shown in Equation (52). Hence, we now compute only the general expression of  $\underline{x}_p(t)$ .

#### 3.1 Frequency response matrix

The frequency response matrix can be obtained considering an harmonic force applied to the system ( $F(t) = F_0 e^{i\Omega t}$ ). Given the general solution, we can compute its derivatives:

$$\underline{x}_p = \underline{X}_{p0} e^{i\Omega t} \quad \dot{\underline{x}}_p = i\Omega \underline{X}_{p0} e^{i\Omega t} \quad \ddot{\underline{x}}_p = -\Omega^2 \underline{X}_{p0} e^{i\Omega t} \quad (58)$$

Substituting them into the first equation of the system (56) and removing the dependence from time, we can get to the expression:

$$\underline{X}_{p0} = [-\Omega^2[M^*] + i\Omega[C_R^*] + [K^*]]^{-1} \underline{F}_0 \quad (59)$$

that can also be written highlighting the mechanical impedance matrix  $[D(\Omega)]$ , whose inverse coincides with the frequency response matrix.

$$\underline{X}_{p0} = [D(\Omega)]^{-1} \underline{F}_0 \quad \underline{X}_{p0} = [H(\Omega)] \underline{F}_0 \quad (60)$$

Consequently the  $H_{ij}$  values will be defined as:

$$H_{ij} = \frac{X_{p0i}}{F_{0j}} \quad (61)$$

The resulting  $H_{ij}$  are reported in figures below.

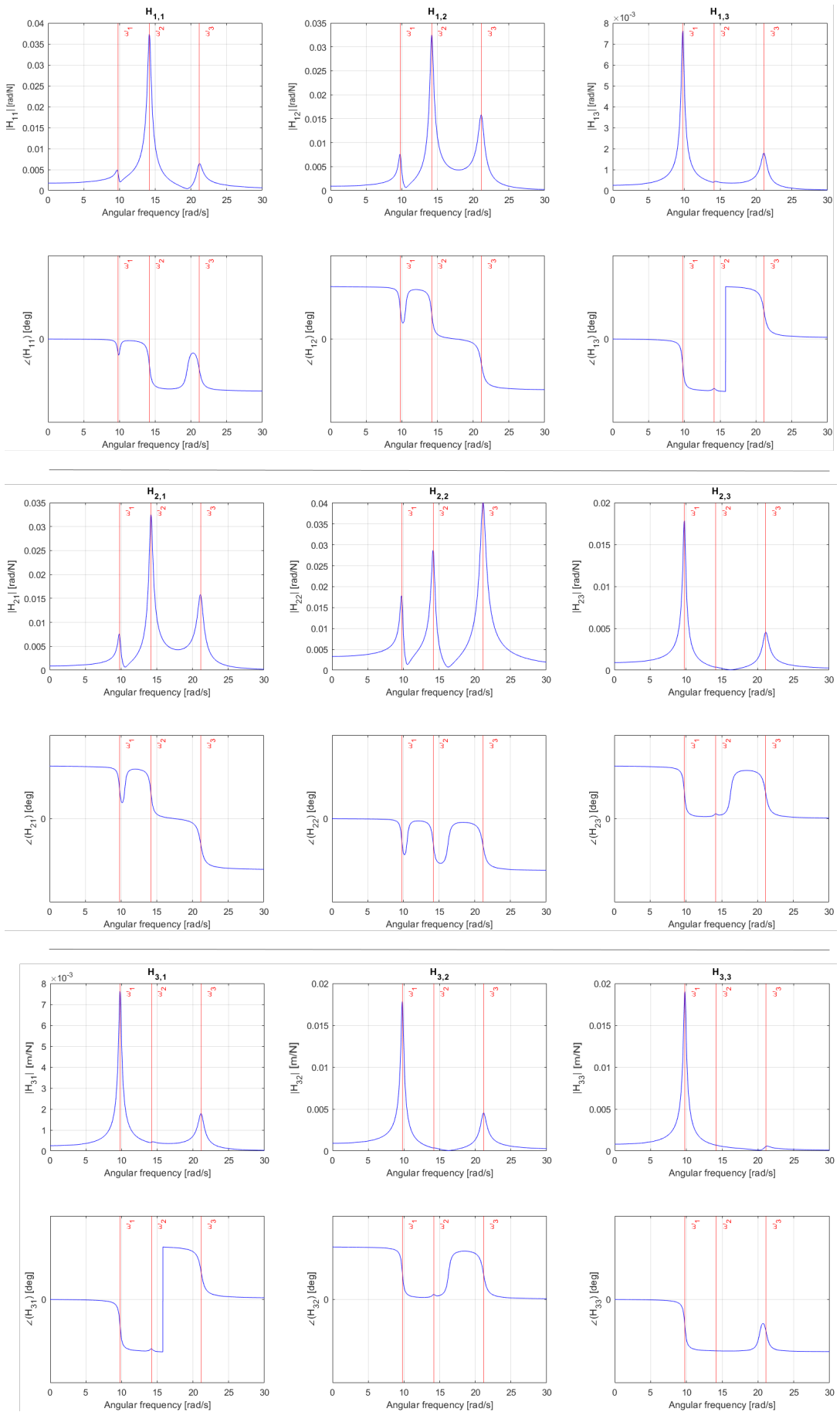


Figure 4: Frequency Response Functions for phase and amplitude.

### 3.2 Co-located FRF in A

The co-located Frequency Response Function in a point relates the response of that point of the system, in this case a displacement, with the cause, a force applied in the same point. In order to do so, we need to express the displacement of the point A as a function of the independent variables through an appropriate matrix transformation i.e. it's Jacobian  $[\Lambda_A]$ :

$$[\Lambda_A] = \begin{bmatrix} 0 \\ R_2 \\ 1 \end{bmatrix} \quad (62)$$

The effect of the force applied in A on the independent variables previously chosen can be calculated as:

$$[H_{iA}(\Omega)] = [H(\Omega)] [\Lambda_A] \quad (63)$$

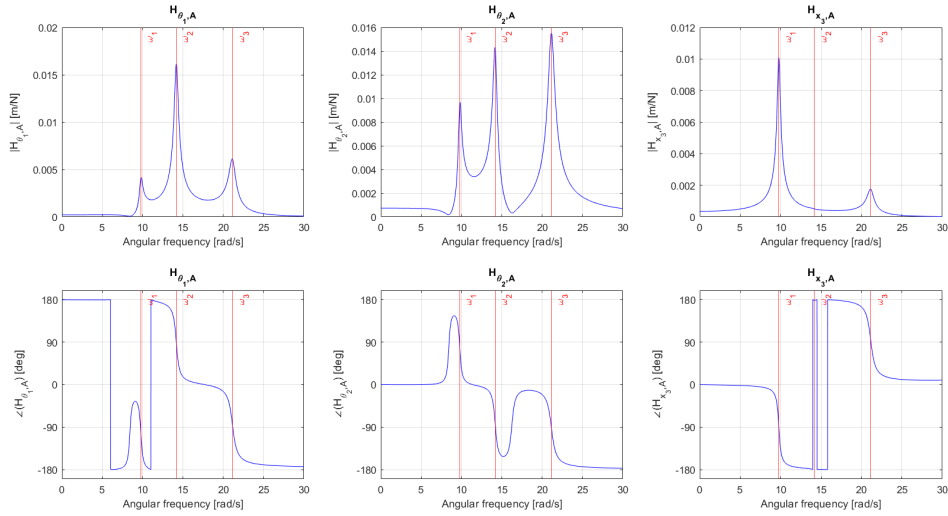


Figure 5: Effects of the force applied in A on  $\theta_1$ ,  $\theta_2$ ,  $x_3$ .

The correspondent co-located FRF in the point A which relates  $x_A$  with  $F_A$  will then be computed as follows:

$$H_{x_A,A}(\Omega) = [\Lambda_A]^T [H(\Omega)] [\Lambda_A] \quad (64)$$

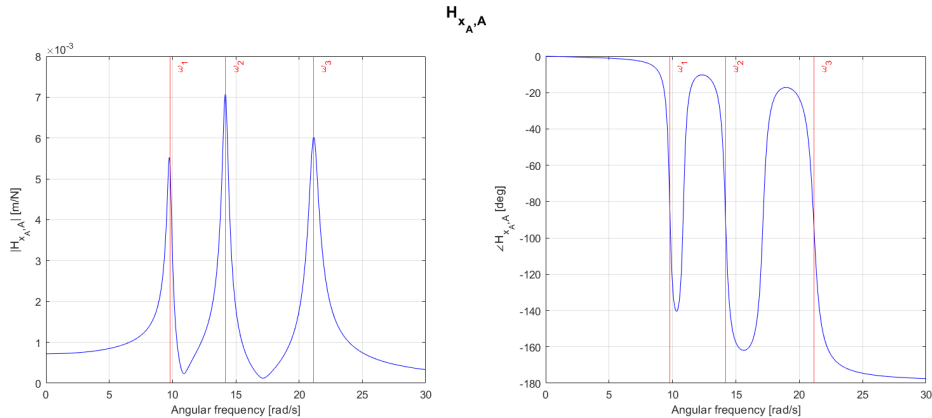


Figure 6: Co-located FRF in the point A.

### 3.3 Co-located FRF for $\theta_2$

The procedure for determining the co-located FRF relative to the rotation of the disk 2  $\theta_2$  in relation to a torque applied to the same disk  $C_2$  is the same as before. First we define the Jacobian

$[\Lambda_{\theta_2}]$  which is clear to depend only on the independent variable  $\theta_2$  itself:

$$[\Lambda_{\theta_2}] = \begin{bmatrix} 0 \\ 1 \\ 0 \end{bmatrix} \quad (65)$$

Repeating the other calculations as before we get the following graphs respectively for the independent variables-torque  $C_2$  relation and for the actual co-located FRF which relates  $\theta_2$  with  $C_2$ .

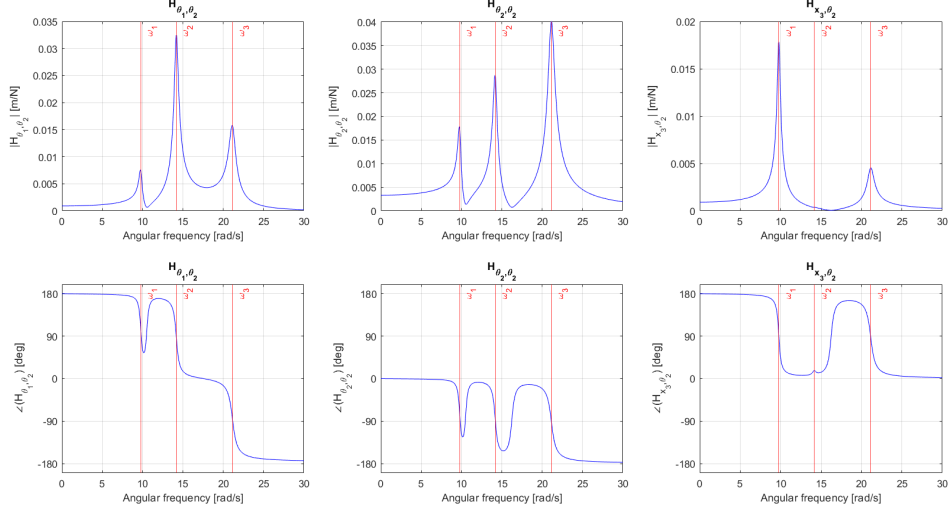


Figure 7: Effects of the torque applied on the disk  $M_2$  on  $\theta_1$ ,  $\theta_1$ ,  $x_3$ .

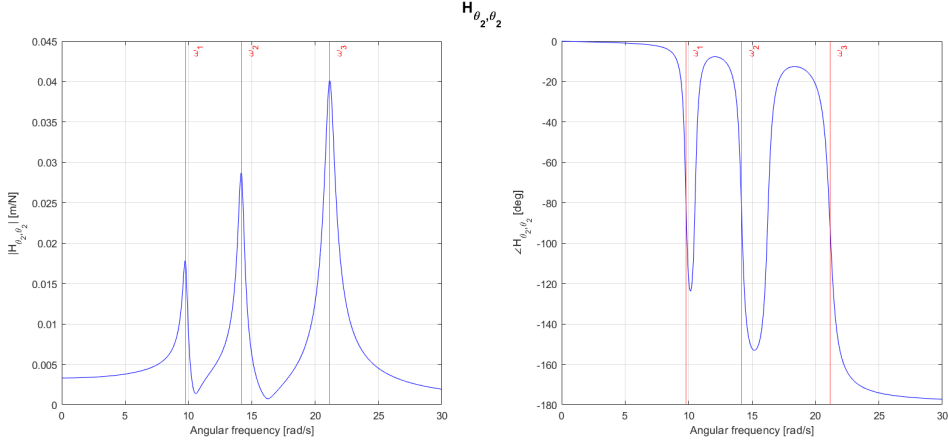


Figure 8: Co-located FRF w.r.t. the rotation  $\theta_2$ .

### 3.4 Complete time response

We now need to evaluate the complete response, highlighting its transient and steady-state components when the system is excited by the following force which is plotted in figure (9) :

$$F(t) = F_1 + F_2 = A_1 \cos(2\pi f_1 t) + A_2 \cos(2\pi f_2 t), \quad \begin{cases} A_1 = 15 [N] \\ f_1 = 1.5 [Hz] \\ A_2 = 7 [N] \\ f_2 = 3.5 [Hz] \end{cases} \quad (66)$$

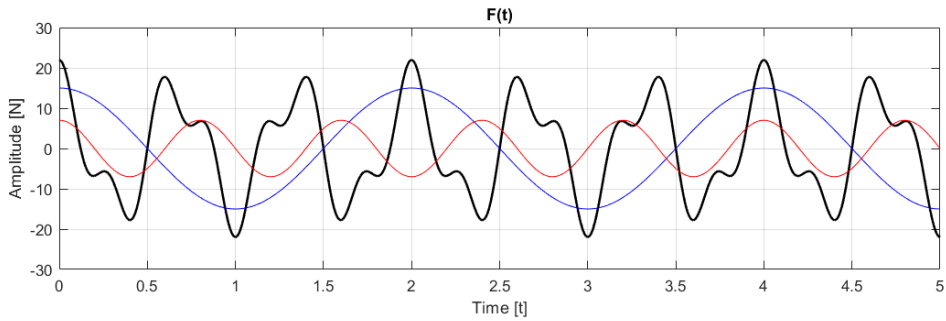


Figure 9:  $F(t)$  and its harmonic components  $F_1$  and  $F_2$

As previously mentioned in the introduction of section (3), in order to obtain a comprehensive description of the forced system, it is necessary to derive the solution as a combination of the general solution  $x_g$  and the particular solution  $x_p$ . The general solution represents the free response of the damped system, which has already been calculated in section (2) (i.e., the zero-input response). On the other hand, the particular solution refers to the steady-state response. The steady-state response (SSR) is the system's response when it reaches a state of equilibrium, where the contribution from the zero-input response has finished.

In order to evaluate the particular solution  $x_p$  we can use the superposition of effects applied to the two components  $F_1(t)$  and  $F_2(t)$  of the force. In particular we'll calculate the solution by using the FRF calculated in section (3.2) since the force is applied in A:

$$\underline{x}_p(t) = [H_{iA}(\Omega_1)]F_1(t) + [H_{iA}(\Omega_2)]F_2(t) \quad (67)$$

The SSR will be periodic with the same period of the excitation force. Finally the complete response can be obtained as:

$$\underline{x}(t) = \underline{x}_g(t) + \underline{x}_p(t) \quad (68)$$

In the following figures we exploit the complete response and its transient and steady-state components.

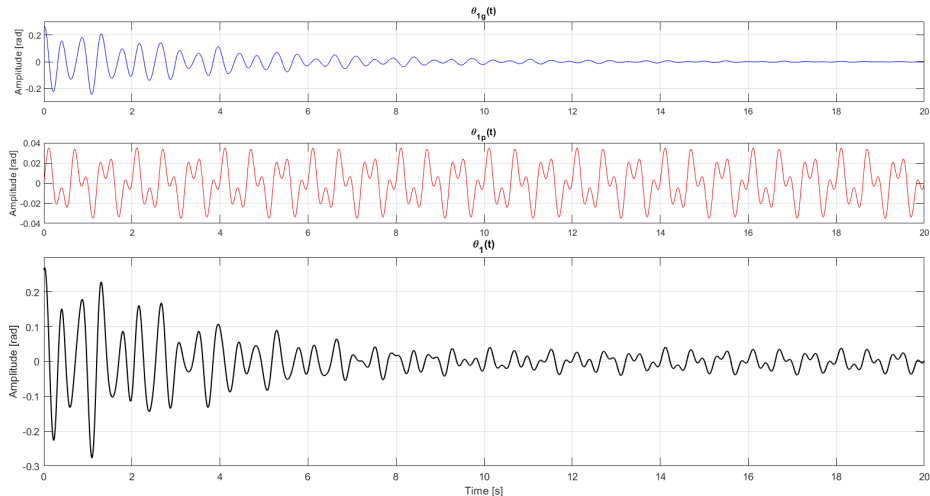


Figure 10:  $\theta_1$  free response, steady-state response and total response.

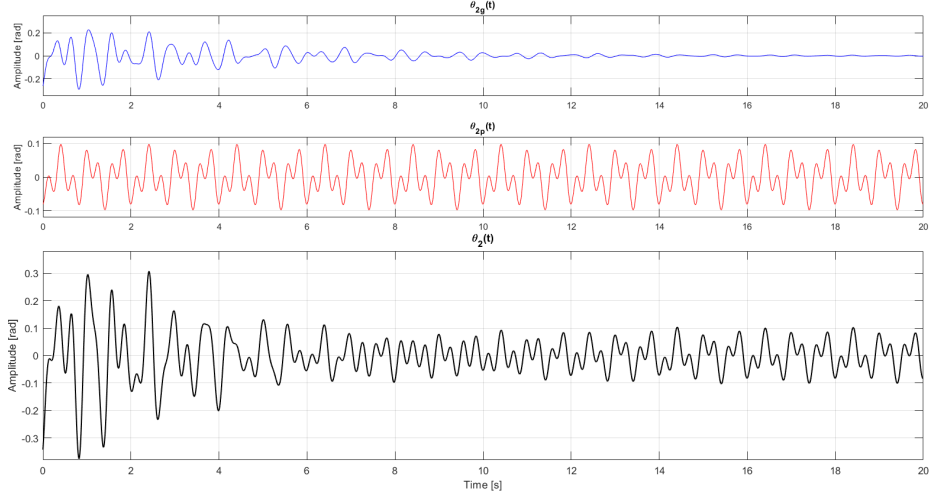


Figure 11:  $\theta_2$  free response, steady-state response and total response.

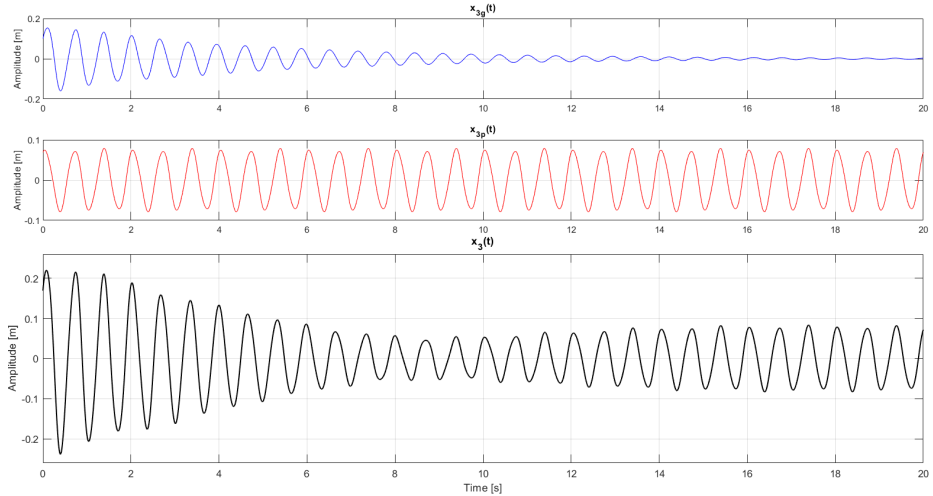


Figure 12:  $x_3$  free response, steady-state response and total response.

### 3.5 Steady-state response of a periodic triangular wave

Subsequently we consider a force  $F(t)$  with a periodic triangular waveform of fundamental frequency  $f_0$  applied in A:

$$F(t) = \frac{8}{\pi^2} \sum_{k=0}^4 (-1)^k \frac{\sin[(2k+1)2\pi f_0 t]}{(2k+1)^2} \quad (69)$$

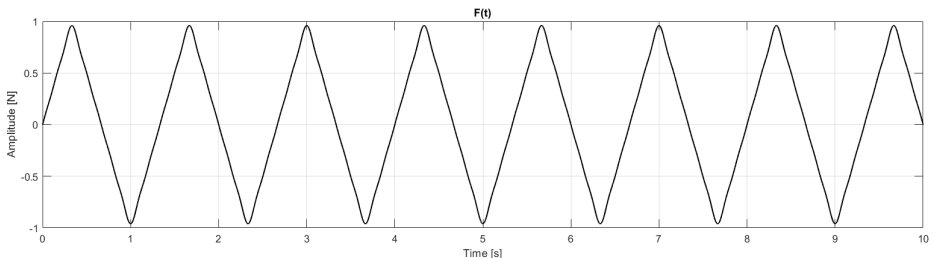


Figure 13:  $F(t)$  triangular wave.

Now we will calculate the steady state response of the displacement  $x_A$  using the transformation matrix that we previously calculated in section (3.2):

$$H_{x_A A}(\Omega) = [\Lambda_A]^T [H(\Omega)] [\Lambda_A] \quad (70)$$

$$x_A(t) = H_{x_A A}(2\pi f_0) F(t) \quad (71)$$

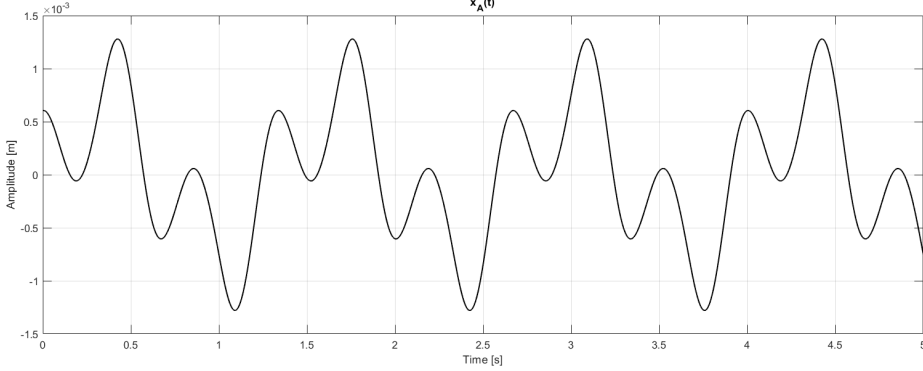


Figure 14:  $x_A(t)$  steady-state response.

## 4 Modal approach

In this section we will study the system using the modal approach. The fundamental relationship that we will use is the following, which relates the vector of the independent variables  $\underline{x}$  to the vector of modal coordinates  $\underline{q}$ :

$$\begin{cases} \underline{x} = [\Phi] \underline{q} \\ \dot{\underline{x}} = [\Phi] \dot{\underline{q}} \\ \ddot{\underline{x}} = [\Phi] \ddot{\underline{q}} \\ \delta \underline{x} = [\Phi] \delta \underline{q} \end{cases} \quad (72)$$

$[\Phi]$  is the matrix containing the mode shapes computed in the first section considering the Rayleigh damping:

$$[\Phi] = \begin{bmatrix} \underline{X}^{(I)} \\ \underline{X}^{(II)} \\ \underline{X}^{(III)} \end{bmatrix} \quad (73)$$

### 4.1 Equations of motion in modal coordinates

Now we can rewrite all the components of the Lagrange equation using the relations described:

$$E_k = \frac{1}{2} \dot{\underline{x}}^T [M^*] \dot{\underline{x}} = \frac{1}{2} \dot{\underline{q}}^T [\Phi]^T [M^*] [\Phi] \dot{\underline{q}} = \frac{1}{2} \dot{\underline{q}}^T [M_q] \dot{\underline{q}} \quad (74)$$

$$\begin{cases} [M_q] = [\Phi]^T [M] [\Phi] \\ [K_q] = [\Phi]^T [K] [\Phi] \\ [C_q] = \alpha [M_q] + \beta [K_q] \\ Q_q = [\Phi]^T F_x \end{cases} \quad (75)$$

Given the matrices computed above, the equation of the free motion of the system expressed in modal coordinates becomes:

$$[M_q] \ddot{\underline{q}} + [C_q] \dot{\underline{q}} + [K_q] \underline{q} = 0 \quad (76)$$

With the same procedure used in section (3.1) we now compute and plot the Modal Frequency Response Matrix  $H_q(\Omega)$  in terms of magnitude and phase.

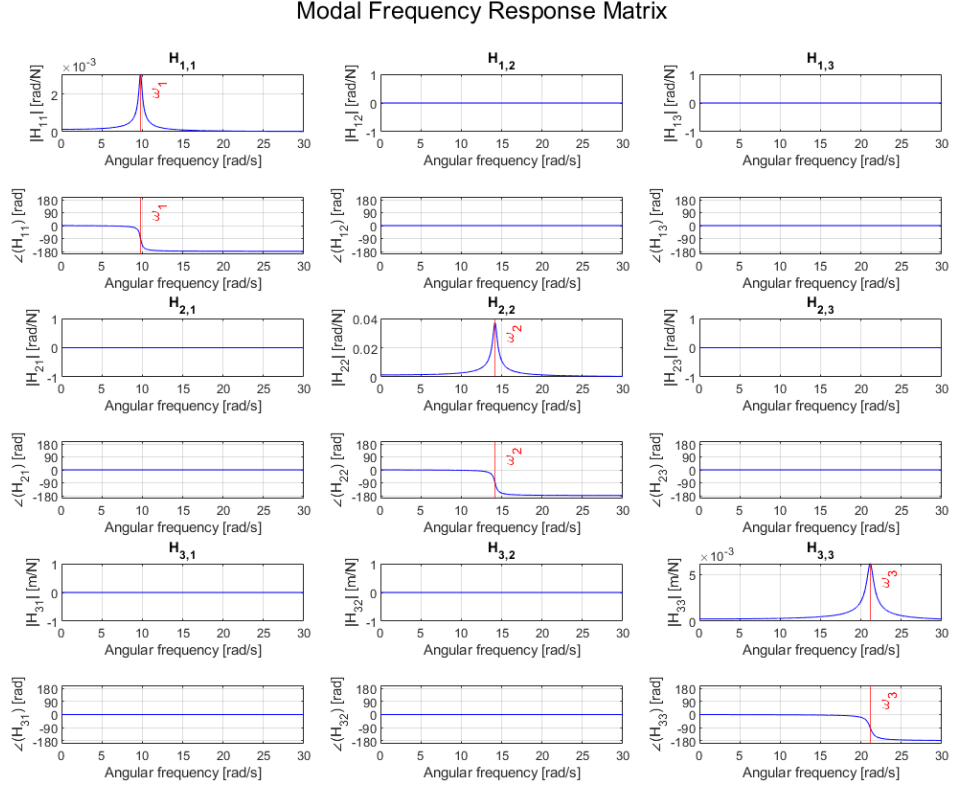


Figure 15: FRF magnitude and phase for modal coordinates.

As expected the only non-zero elements of the matrix are the diagonal terms, because of the orthogonality of the modal coordinates.

## 4.2 Co-located FRF Reconstruction of point A

With this kind of representation of the system, it is possible to see how each mode contributes to the total movement of the system: an example of this is the reconstruction of the FRF in A. The three FRFs, one for each degree of freedom can be expressed in terms of the superposition of the modal FRFs:

$$[H_{iA}(\Omega)] = [\Phi]^T [H_q(\Omega)] [\Phi] [\Lambda_A] \quad (77)$$

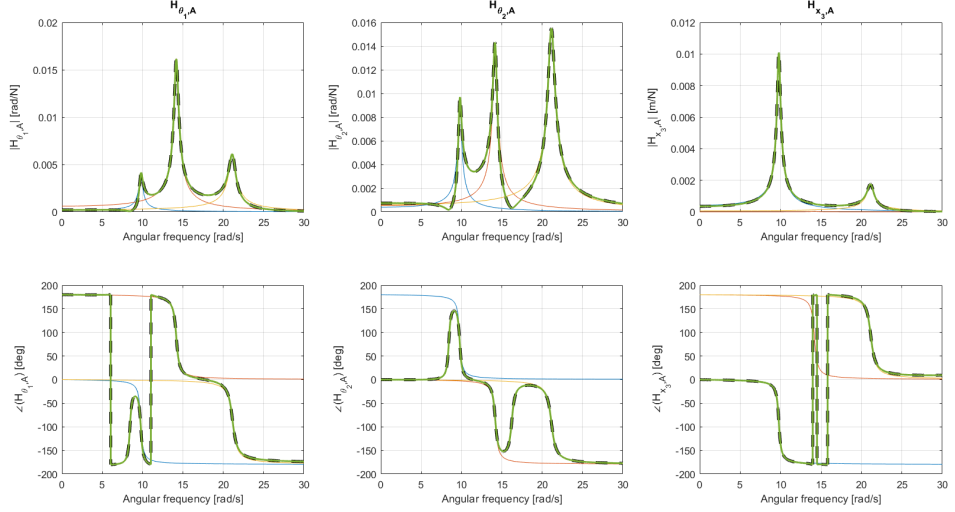


Figure 16:  $H_{x_i,A}(\Omega)$  reconstructed co-located FRF using modal approach and its components compared with the physical coordinates co-located FRF.

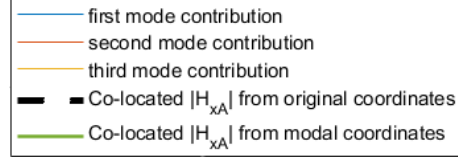


Figure 17: Legend of figure (16)

The graphs above show a complete overlap between the FRFs we found earlier through physical coordinates, and the reconstruction of them achieved with a modal approach. Each modal FRF, scaled by the coefficient contained in the corresponding mode shape, approximates well the considered function around its resonating frequency. The sum of the three approximations yields a perfect reproduction of the original FRFs.

Now we can calculate the correspondent co-located FRF in the point A using transformation matrix that we previously calculated in section (3.2):

$$H_{x_A,A}(\Omega) = [\Lambda_A]^T [H_{iA}(\Omega)] = [\Lambda_A]^T [\Phi]^T [H_q(\Omega)] [\Phi] [\Lambda_A] \quad (78)$$

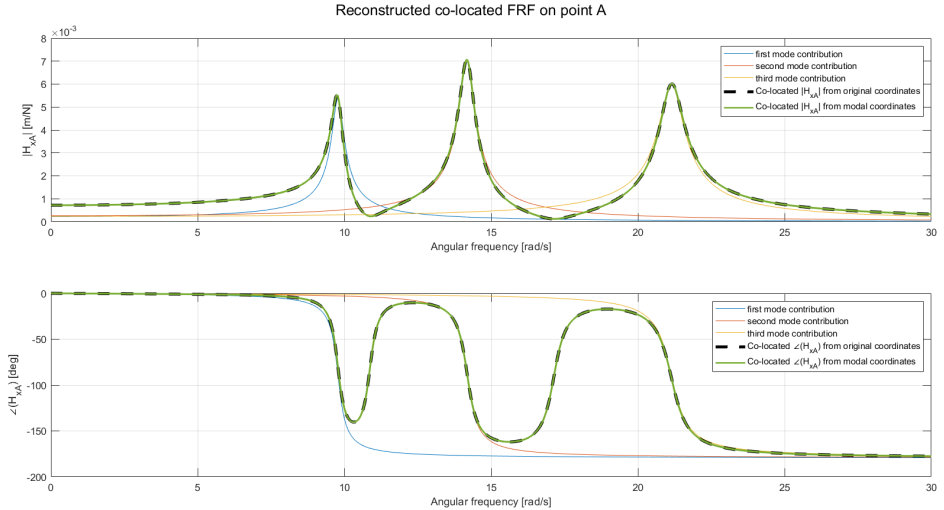


Figure 18:  $H_{x_A,A}(\Omega)$  reconstructed co-located FRF using modal approach and its components compared with the physical coordinates co-located FRF.

### 4.3 Co-located FRF Reconstruction for $\theta_2$

In the same way we can use the Jacobian related to  $\theta_2$  calculated in section 3.3 in order to rebuild the co-located FRF for  $\theta_2$ :

$$H_{\theta_2\theta_2}(\Omega) = [\Lambda_{\theta_2}]^T [H_{i\theta_2}(\Omega)] \quad (79)$$

In this case we plot directly the  $H_{\theta_2\theta_2}(\Omega)$  avoiding the graphs of the effect on the independent variables. This is because the plots for the independent variables will be empty except for  $H_{22}(\Omega)$ , i.e. the one referring to  $\theta_2$  which is clearly coincident with  $H_{\theta_2}(\Omega)$ .

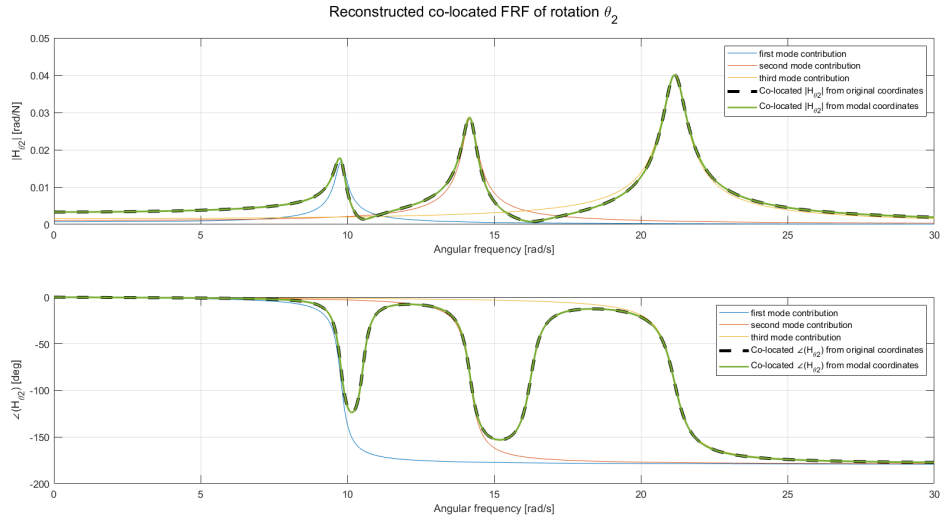


Figure 19:  $H_{\theta_2,\theta_2}(\Omega)$  reconstructed co-located FRF using modal approach and its components compared with the physical coordinates co-located FRF.

### 4.4 Steady state amplitude of response

We now want to evaluate the steady state amplitude of response for the three degrees of freedom when excited by a horizontal force applied in A using only the first mode. In order to do so, we can follow the procedure of section (4.2) after adjusting the  $[\phi]$  matrix in order to consider only the first mode (eigenvector):

$$[\Phi] = \begin{bmatrix} \underline{X}^{(I)} \\ 0 \\ 0 \end{bmatrix} \quad (80)$$

After recalculating the  $H_q(\Omega)$  matrix, which representation is omitted because of its intuitiveness, we plot the approximated  $[H_{iA}(\Omega)]$  using only the first mode with the relation (77).

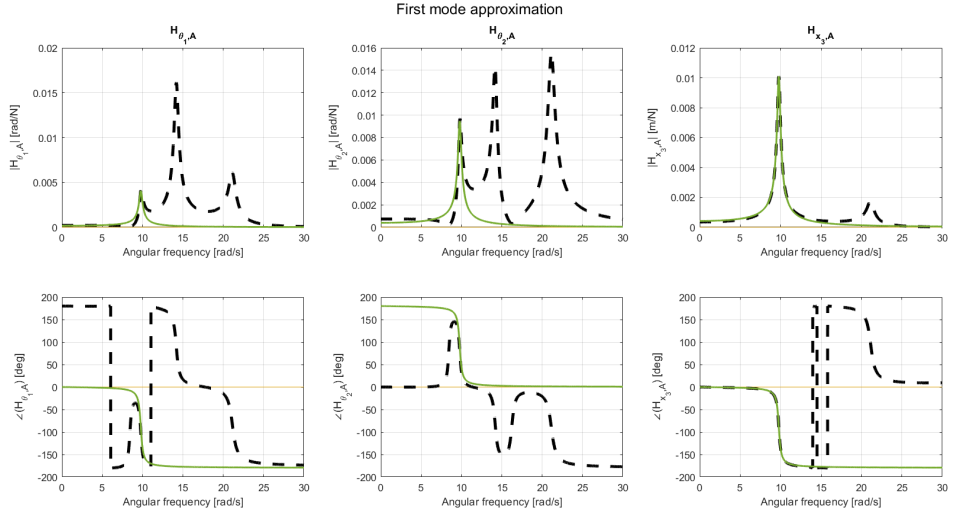


Figure 20:  $[H_{iA}(\Omega)]$  reconstructed co-located FRF using only the first mode. Legend in Fig.(17).

As we can see from the figures, the approximation works well for frequencies before or close to the first vibrating mode. For higher frequencies the approximation damps the response with respect to the real FRF.

Let's now evaluate the complete response for two harmonic forces  $F_1(t)$ , with frequency of 1.5Hz close to the first vibrating mode, and  $F_2(t)$  with frequency of 3.5Hz. To do so, we follow the passages of section (3.4).

$$\underline{x}_p(t) = [H_{iA}(\Omega_1)]F_1(t) \quad (81)$$

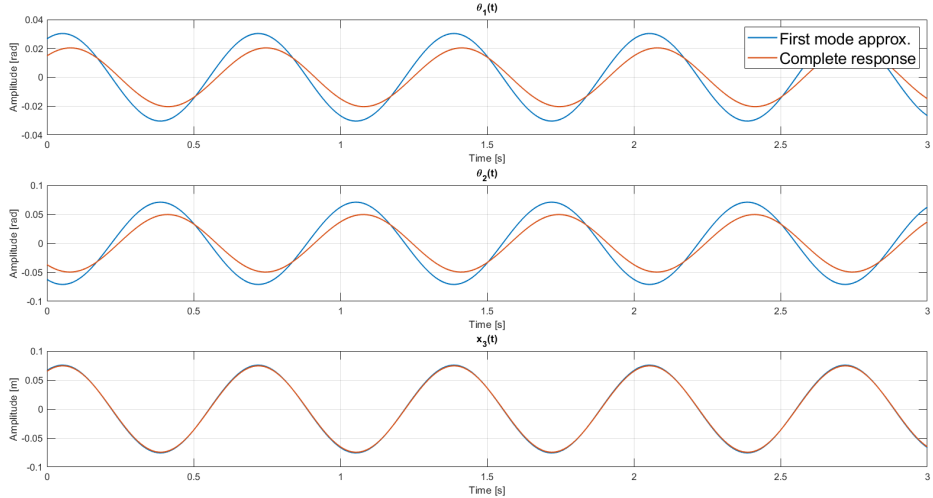


Figure 21:  $\theta_1$  SSR approximated with the first mode only compared to its non-approximated trend.

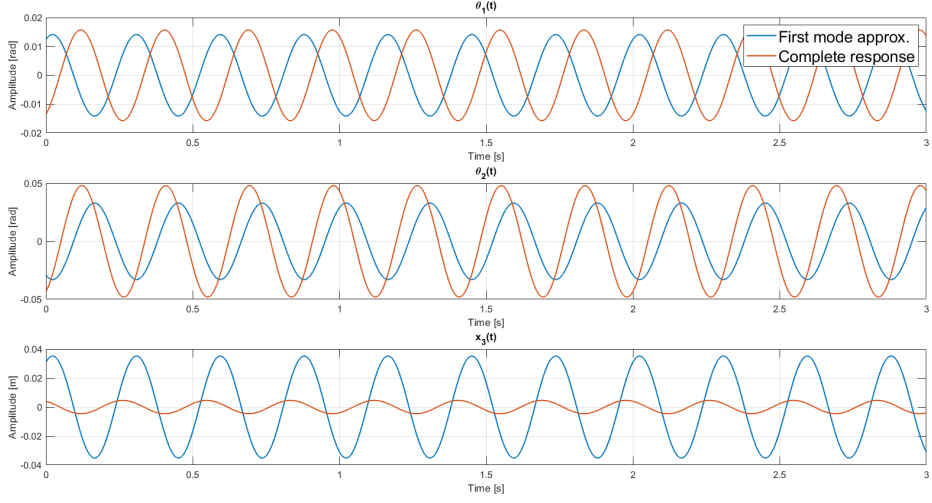


Figure 22:  $\theta_2$  SSR approximated with the first mode only compared to its non-approximated trend.

As we expected the graphs highlight that the reconstruction for  $f_1$ , which is close to the first mode, is quite good, while for  $f_2$  the differences between the approximated and real trend are more evident. In particular we can observe it clearly by looking at the independent variable  $x_3$  which is the one that depends the most on the first mode, as we already discussed in section 2.1.

## 5 Optional

### 5.1 Graphical representation of the mode shapes

Using the eigenvectors  $\underline{X}^{(i)}$  and their linked eigenvalues  $\omega_i$  (the characteristic frequencies of the modes) obtained in section 1.6, we can compute the displacement of each free coordinate relative to each single vibration mode of the system:

$$r_i(t) = \underline{X}^{(i)} \sin(\omega_i t) \quad (82)$$

We can represent the displacements with sinusoidal graphs:

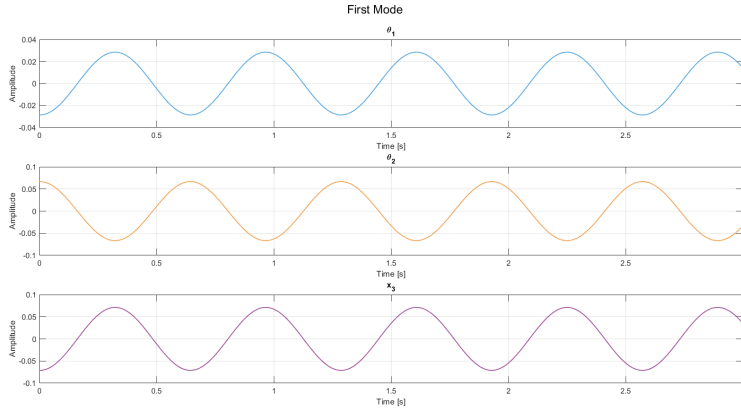


Figure 23: First mode shapes representation.

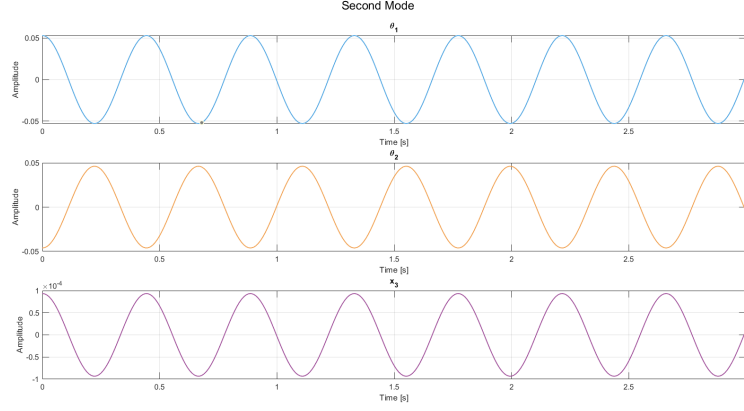


Figure 24: Second mode shapes representation.

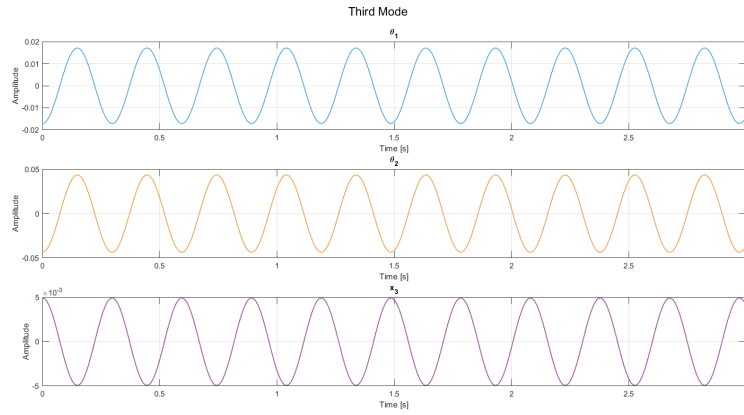


Figure 25: Third mode shapes representation.

## 5.2 FRF representation using different diagrams

Now we will represent one element of the Frequency Response Matrix  $H(\Omega)$  computed in section (3.1) as superposition of the modal frequency response functions and we will compare these results to the original diagram of (4) but considering different types of diagrams:

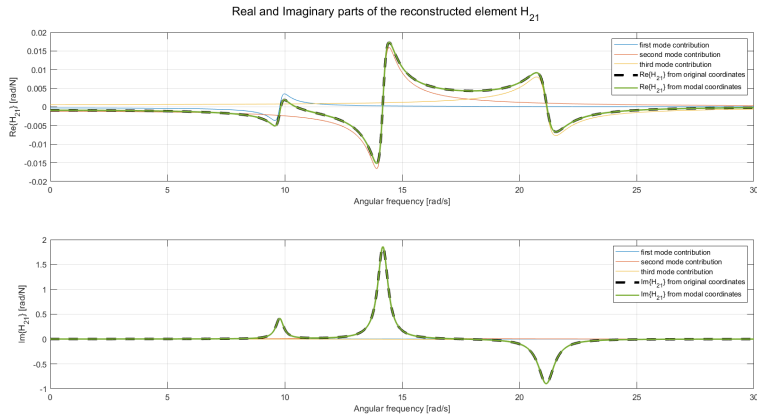


Figure 26: Real and imaginary parts of reconstructed element  $H_{21}$



# POLITECNICO MILANO 1863

Homework nr.3 Vibration Analysis and Vibroacoustics 22/23

Riccardo Iaccarino, Rocco Scarano, Enrico Dalla Mora

June 27, 2023

## Contents

|          |  |           |
|----------|--|-----------|
| <b>1</b> | <b>Experimental Frequency Response Functions</b> | <b>3</b>  |
| <b>2</b> | <b>Modal Parameters</b>                          | <b>4</b>  |
| 2.1      | Natural Frequencies . . . . .                    | 4         |
| 2.2      | Adimensional Damping Ratios . . . . .            | 4         |
| 2.3      | Modal Damping . . . . .                          | 4         |
| 2.4      | Mode Shapes Approximation . . . . .              | 5         |
| <b>3</b> | <b>Modal Parameters Identification</b>           | <b>6</b>  |
| <b>4</b> | <b>Modal Parameters Comparison</b>               | <b>8</b>  |
| <b>5</b> | <b>Modal Approach FRF Reconstruction</b>         | <b>9</b>  |
| <b>6</b> | <b>Co-located FRF in <math>x_2</math></b>        | <b>11</b> |
| <b>7</b> | <b>System Matrices</b>                           | <b>12</b> |

## Time Responses

Given the dataset of the time responses for the displacements  $x_1, x_2, x_3$  and  $x_4$  when exited by a force  $F$ , we first plot the time trends as to visualize and understand how these responses behave. Note that the samples are collected by the four sensors with a sampling period of  $d_t = 0.001$  [s].

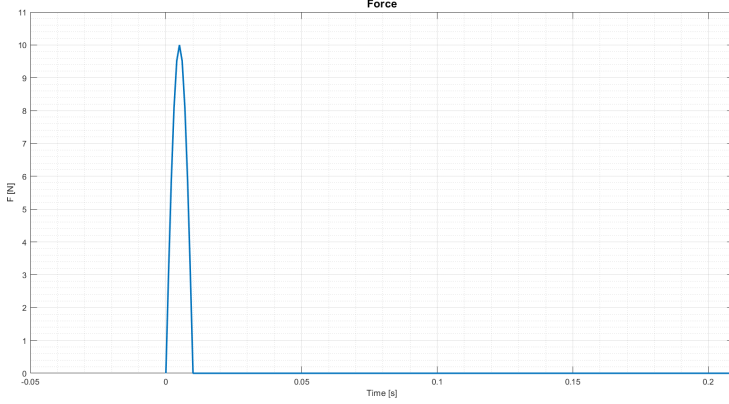


Figure 1: Impulsive behaviour of the force  $F$ .

As we can see from figure (1) the force is impulsive and therefore the system is fully characterized by its free response. This means the system response is a transient since the system is real and therefore damped.

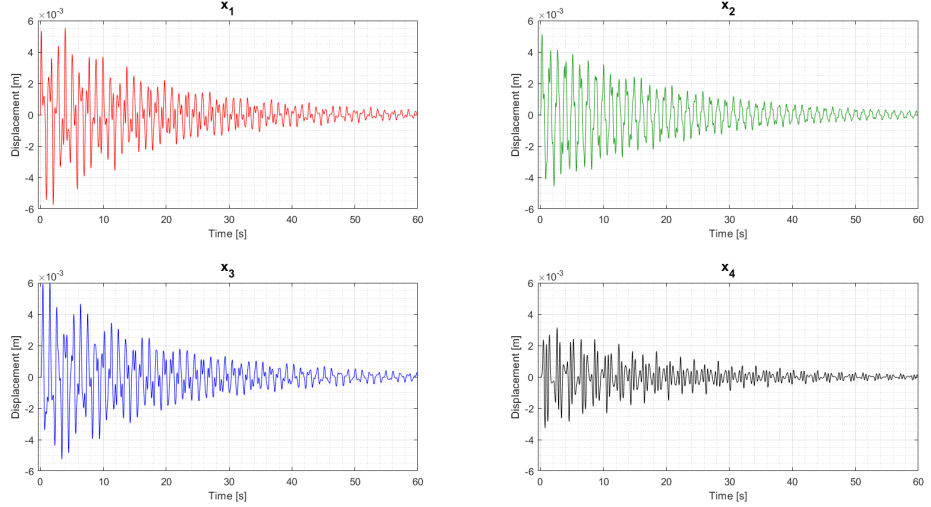


Figure 2: Time responses of  $x_1, x_2, x_3$  and  $x_4$ .

# 1 Experimental Frequency Response Functions

In order to compute the experimental Frequency Response Function we first need to translate to the frequency domain. In order to do so, we employ the Fast Fourier Transform of which we considered only the positive frequencies being the signal real-valued. At this point, the experimental frequency response function of the system can be computed as the ratio between the complex spectrum of the displacements and the one relative to the input force:

$$H_{jk}^{exp}(\Omega) = \frac{X_j(\Omega)}{F(\Omega)} \quad (1)$$

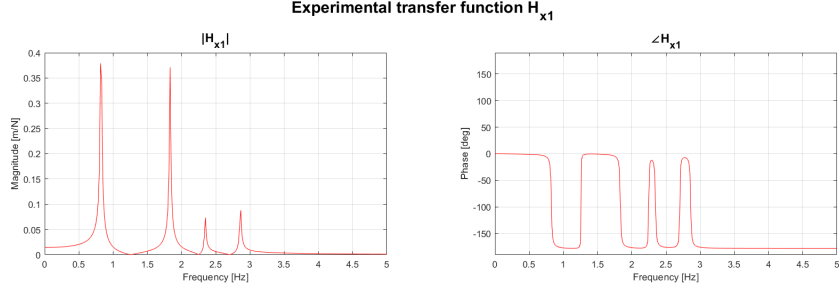


Figure 3:  $x_1$  experimental FRF.

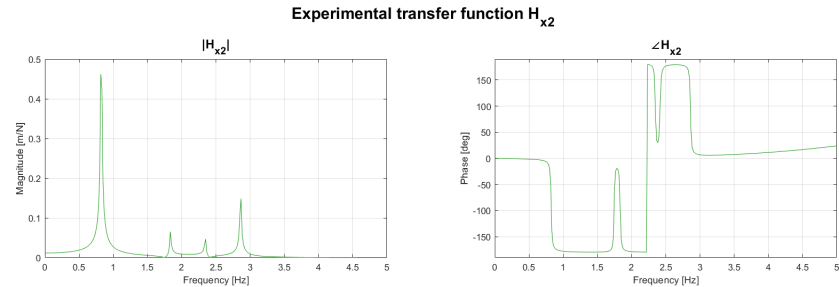


Figure 4:  $x_2$  experimental FRF.

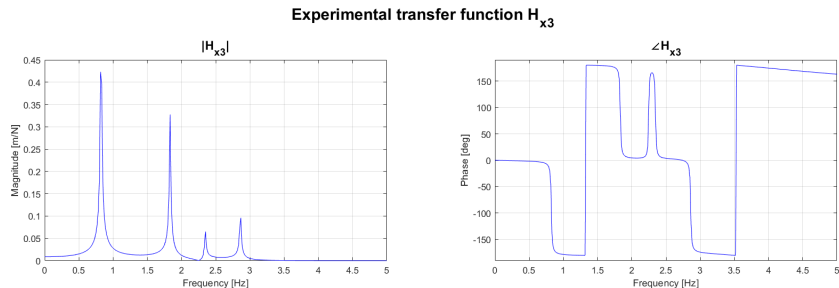


Figure 5:  $x_3$  experimental FRF.

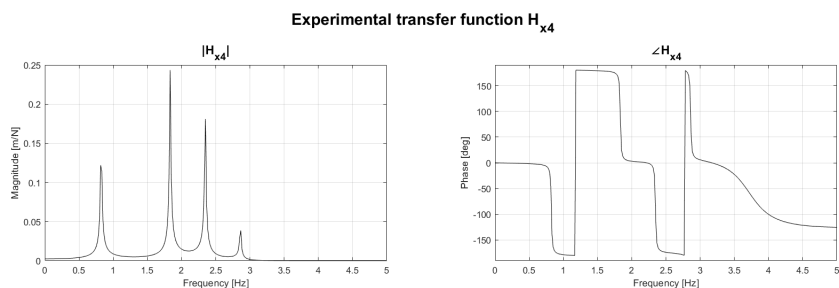


Figure 6:  $x_4$  experimental FRF.

## 2 Modal Parameters

### 2.1 Natural Frequencies

First of all we search for the natural frequencies by computing the local maxima for each FRF. The maxima will be placed in correspondence of the natural frequencies of the system. After doing so we figured out that this method is quite reliable, since the values don't change between the various FRFs. It's possible to see in the matrix below:

$$[f_0] = \begin{bmatrix} 0.8167 & 1.8333 & 2.3500 & 2.8666 \\ 0.8167 & 1.8333 & 2.3500 & 2.8666 \\ 0.8167 & 1.8333 & 2.3500 & 2.8666 \\ 0.8167 & 1.8333 & 2.3500 & 2.8666 \end{bmatrix} [\text{Hz}] \quad (2)$$

We can now estimate the natural frequencies  $\omega_{0ij} = 2\pi f_{0ij}$ .

$$[\omega_0] = \begin{bmatrix} 5.1312 & 11.5190 & 14.7652 & 18.0115 \\ 5.1312 & 11.5190 & 14.7652 & 18.0115 \\ 5.1312 & 11.5190 & 14.7652 & 18.0115 \\ 5.1312 & 11.5190 & 14.7652 & 18.0115 \end{bmatrix} [\text{rad/s}] \quad (3)$$

### 2.2 Adimensional Damping Ratios

In order to evaluate the adimensional damping ration  $h_i$  we can use two different methods: "the Half-power method" ( $h_i = \frac{(\omega_2)^2 - (\omega_1)^2}{4(\omega_i)^2}$ ) or the "Derivative of the FRF phase method". We will use the second one since the system is underdamped (more generally, lightly damping) and the natural frequencies are well separated. Under this hypothesis, we can assert that in a narrow frequency band about each natural frequency the resonating modal component prevails over the others:

$$h_i = -\frac{1}{w_{0i} \frac{\partial \angle(H_k)^{\text{exp}}}{\partial \Omega} \Big|_{\Omega=\omega_{0i}}} \quad (4)$$

$$[h] = \begin{bmatrix} 0.0195 & 0.0081 & 0.0064 & 0.0054 \\ 0.0195 & 0.0082 & 0.0066 & 0.0053 \\ 0.0195 & 0.0081 & 0.0064 & 0.0053 \\ 0.0195 & 0.0081 & 0.0064 & 0.0053 \end{bmatrix} \quad (5)$$

As we can see in this case there are minimal differences in the order of  $10^{-5}$  which we can consider negligible. It's possible to notice something interesting looking at this matrix and at the experimental FRF graph: the adimensional damping ratios decrease for higher natural frequencies, this is clear looking specifically to the first two peaks of the transfer functions, the first one, corresponding to an higher  $h$ , is smoother than the second one.

### 2.3 Modal Damping

Now we proceed computing the modal damping employing the following relation:

$$c_{qi} = -\frac{2}{\frac{\partial \angle H_k}{\partial \Omega} \Big|_{\Omega=\omega_{0i}}} = 2h_i \omega_i \quad (6)$$

we get the following values:

$$[c] = \begin{bmatrix} 0.1998 & 0.1862 & 0.1895 & 0.1929 \\ 0.1997 & 0.1887 & 0.1954 & 0.1927 \\ 0.1997 & 0.1863 & 0.1901 & 0.1923 \\ 0.1997 & 0.1862 & 0.1883 & 0.1919 \end{bmatrix} \quad (7)$$

As was already possible to see in the matrix, the measurement that moves away the most from the others is the second one, in particular in the damping value associated with the third mode shape. This may be caused by Matlab approximations.

## 2.4 Mode Shapes Approximation

It's now possible to approximate the mode shapes which will form the modal matrix  $[\Phi_0]$ . The FRF of a system is defined as the linear combination of the single DOF's FRFs, so it can be approximated to just one of these contribution if we refer to a limited frequency range. In particular, if the system respects the hypothesis of low damping and well-separated natural frequencies, we have two different possibilities:

$$H_{jk}^{exp}(\Omega) \approx H_{jk}^{num}(\Omega) = \frac{A_j + jB_j}{-\Omega^2 m_{qi} + j\Omega c_{qi} + k_{qi}} + (C_j + jD_j) + \left( \frac{E_j + jF_j}{\Omega^2} \right) \quad (8)$$

$$H_{jk}^{exp}(\Omega) = \frac{X_j^{(i)} X_k^{(i)}}{-\Omega^2 m_{qi} + j\Omega c_{qi} + k_{qi}} = \frac{X_j^{(i)} X_k^{(i)}}{-\Omega^2 m_{qi} + j\Omega m_{qi} h_i \omega_0 i + k_{qi}} \quad (9)$$

The first approach can be divided into 3 terms accounting for different regions of the modal component:

- $\frac{A_j + jB_j}{-\Omega^2 m_{qi} + j\Omega c_{qi} + k_{qi}}$  is accounting for the resonating modal component;
- $(C_j + jD_j)$  is accounting for the quasi-static region of the other modal components resonating at higher frequencies;
- $\left( \frac{E_j + jF_j}{\Omega^2} \right)$  is accounting for the seismographic region of the other modal components resonating at lower frequencies.

The second method is less accurate, since it basically refers to just the first term of the other approach. Nonetheless it will be useful for two purposes: computing the mode shapes and quicken the computation of the unknowns  $c_{qi}, k_{qi}, A_j, B_j, C_j, D_j, E_j, F_j$  (that requires iterative solutions).

We can compute the equation (9) for  $\Omega = \omega_0$ . We also use some relations:  $m_{qi} = 1$ ,  $c_{qi} = 2h_i \omega_i$  and  $k_{qi} = \omega_i^2$ :

$$H_{jk}^{exp}(\Omega = \omega_0 i) = \frac{X_j^{(i)} X_k^{(i)}}{-\omega_{0i}^2 + j\omega_{0i}^2 2h_i + \omega_{0i}^2} = \frac{X_j^{(i)} X_k^{(i)}}{j\omega_{0i}^2 2h_i} \quad (10)$$

$$X_j^{(i)} = -\frac{\omega_{0i} 2h_i \operatorname{Im}\{H_{jk}^{exp}(\omega_0 i)\}}{X_k^{(i)}} \quad (11)$$

We can easily compute the mode shape for the case of collocated measurement  $j = k$ , since the two terms will correspond in the FRF matrix:

$$X_{j=k}^{(i)} = X_k^{(i)} = \sqrt{-\omega_{0i} 2h_i \operatorname{Im}\{H_{jk}^{exp}(\omega_0 i)\}} \quad (12)$$

Considering the hypothesis of lightly damping, we can say that the complex part of the numerator of the first term 8 is negligible w.r.t the real part:

$$A_j + iB_j = X_j^{(i)} X_k^{(i)} \approx A_j = X_j^{(i)} X_k^{(i)} \quad (13)$$

Thanks to the fact that  $X_k^{(i)}$  is constant (since, in the experiment under consideration, the position of application of the force k is fixed while the measurement point j varies), we can compute the other  $X_j^{(i)}$  as:

$$X_k^{(i)} = \sqrt{A_{j=k}} \quad (14)$$

$$X_j^{(i)} = \frac{A_j}{X_k^{(i)}} \quad (15)$$

Finally we can compute the matrix of the  $A_j$ , that will be the only non null set of coefficients, as already discussed.

$$[A] = \begin{bmatrix} 0.2766 & 0.7944 & 0.1885 & 0.2526 \\ 0.3407 & 0.1402 & -0.1307 & -0.4365 \\ 0.3133 & -0.7019 & -0.1673 & 0.2842 \\ 0.0904 & -0.5207 & 0.4745 & -0.1148 \end{bmatrix} \quad (16)$$

Iterating the previous relation for each of the selected frequency ranges and in relation to each of the four sensor's measurement we can obtain the  $[\Phi]$  matrix:

$$[\Phi] = [\underline{X}^{(1)} \quad \underline{X}^{(2)} \quad \underline{X}^{(3)} \quad \underline{X}^{(4)}] = \begin{bmatrix} 0.5260 & 0.8913 & 0.4342 & 0.5026 \\ 0.6478 & 0.1573 & -0.3010 & -0.8685 \\ 0.5957 & -0.7875 & -0.3854 & 0.5654 \\ 0.1719 & -0.5842 & 1.0928 & -0.2284 \end{bmatrix} [m] \quad (17)$$

which can also be normalized w.r.t. the first variable (displacement  $x_1$ ):

$$[\Phi]_{norm} = \begin{bmatrix} 1.0000 & 1.0000 & 1.0000 & 1.0000 \\ 1.2316 & 0.1764 & -0.6932 & -1.7279 \\ 1.1326 & -0.8836 & -0.8875 & 1.1249 \\ 0.3269 & -0.6555 & 2.5167 & -0.4545 \end{bmatrix} [m] \quad (18)$$

### 3 Modal Parameters Identification

In order to evaluate an estimation of the modal parameters we approximate the curve with equation (8) which is a system with eight unknowns which can be solved using the minimal residual method. The minimal residual method is an iterative method based on the minimization of the error (residual) w.r.t. to  $H_{jk}^{exp}(\Omega)$ .

From equation (9) we have a system of  $n_{fi}$   $n_m$  equations, where  $n_{fi}$  is the total number of frequency bins contained in the range under consideration and  $n_m$  is the number of measurement. If  $n_{fi}$  (the number of frequencies in frequency range between  $\Omega_A$  and  $\Omega_B$ ) is sufficiently large the system will be over determined. In order to solve it we can use the "Least square method". We can define the vector of parameters:

$$\underline{x} = \{h_j, w_j, A'_j, B'_j, C'_j, D'_j, E'_j, F_1\} \quad (19)$$

We have to minimize the error of our approximation. In order to do this, we define the reconstruction error relative to a generic FRF with respect to  $j, k$ :

$$\epsilon_{rj}(\Omega) = H_{jk}(\Omega) - H_{jk}^{exp}(\Omega) \quad \forall r = 1, 2, \dots n_{fi} n_m \quad (20)$$

The error will be expressed as a summation of all the square modules of  $\epsilon_{rj}(\Omega)$  for all the  $n_{fi}$  and the  $n_m$ :

$$J(\underline{x}) = \sum_{j=1}^4 \sum_{r=1}^{n_{fi}} |\epsilon_{rj}|^2 = \sum_{j=1}^4 \sum_{r=1}^{n_{fi}} \epsilon_{rj} \epsilon_{rj}* \quad (21)$$

The residual minimization method finds the vector of parameters  $\underline{x}$  that minimizes  $J(\underline{x})$ . The initial vector contains the parameters that were determined via the simplified methods.

When applying the RMM for the first range (corresponding to the first natural frequency) the third term of the numerical approximation was ignored, because we neglect the seismographic zone effect of previous frequencies, to maximize the accuracy of the FRF in our range of interest. In the same way, while computing the RMM solution for the last range (fourth natural frequency) the second term (the quasi static zone effect) was ignored for higher frequencies.

While in the calculation of the  $[\Phi_0]$  matrix with equation (9) (simplified method) we had  $\{h_j, \omega_j, A_j\}$  as variables, this method provides us the unknowns  $\{h_j, \omega_j, A_j, B_j, C_j, D_j, E_j, F_j\}$ . In both cases we assume  $m_j = 1$ . This approach is much more accurate than the first one providing the following values:

$$[\omega'_0] = \begin{bmatrix} 5.1803 & 11.5155 & 14.7447 & 17.9789 \\ 5.1803 & 11.5155 & 14.7449 & 17.9764 \\ 5.1802 & 11.5155 & 14.7443 & 17.9765 \\ 5.1802 & 11.5158 & 14.7441 & 17.9762 \end{bmatrix} [rad/s] \quad (22)$$

$$[h'] = \begin{bmatrix} 0.0096 & 0.0043 & 0.0034 & 0.0029 \\ 0.0097 & 0.0043 & 0.0034 & 0.0028 \\ 0.0097 & 0.0044 & 0.0033 & 0.0028 \\ 0.0097 & 0.0044 & 0.0034 & 0.0027 \end{bmatrix} \quad (23)$$

Now we can re-compute the  $[\Phi]$  matrix with the new modal components:

$$[\Phi'] = [\underline{X}'^{(1)} \quad \underline{X}'^{(2)} \quad \underline{X}'^{(3)} \quad \underline{X}'^{(4)}] = \begin{bmatrix} 0.5200 & 0.6526 & 0.3380 & 0.4396 \\ 0.6409 & 0.1143 & -0.2273 & -0.7433 \\ 0.5898 & -0.5815 & -0.2943 & 0.4824 \\ 0.1704 & -0.4351 & 0.8688 & -0.1950 \end{bmatrix} [m] \quad (24)$$

and its normalized form:

$$[\Phi']_{norm} = \begin{bmatrix} 1.0000 & 1.0000 & 1.0000 & 1.0000 \\ 1.2325 & 0.1752 & -0.6724 & -1.6910 \\ 1.1342 & -0.8911 & -0.8707 & 1.0975 \\ 0.3276 & -0.6667 & 2.5708 & -0.4435 \end{bmatrix} [m] \quad (25)$$

Finally we plot the reconstructed FRFs for each of the measured variables compared to the experimental ones. As we can see from the graphs the reconstruction is very accurate in a range of frequencies close to the natural ones. We can also see that the more  $\Omega$  tends to 0 the more the amplitude tends to diverge. This is due to the  $\Omega^2$  components in the denominators of equation (8).

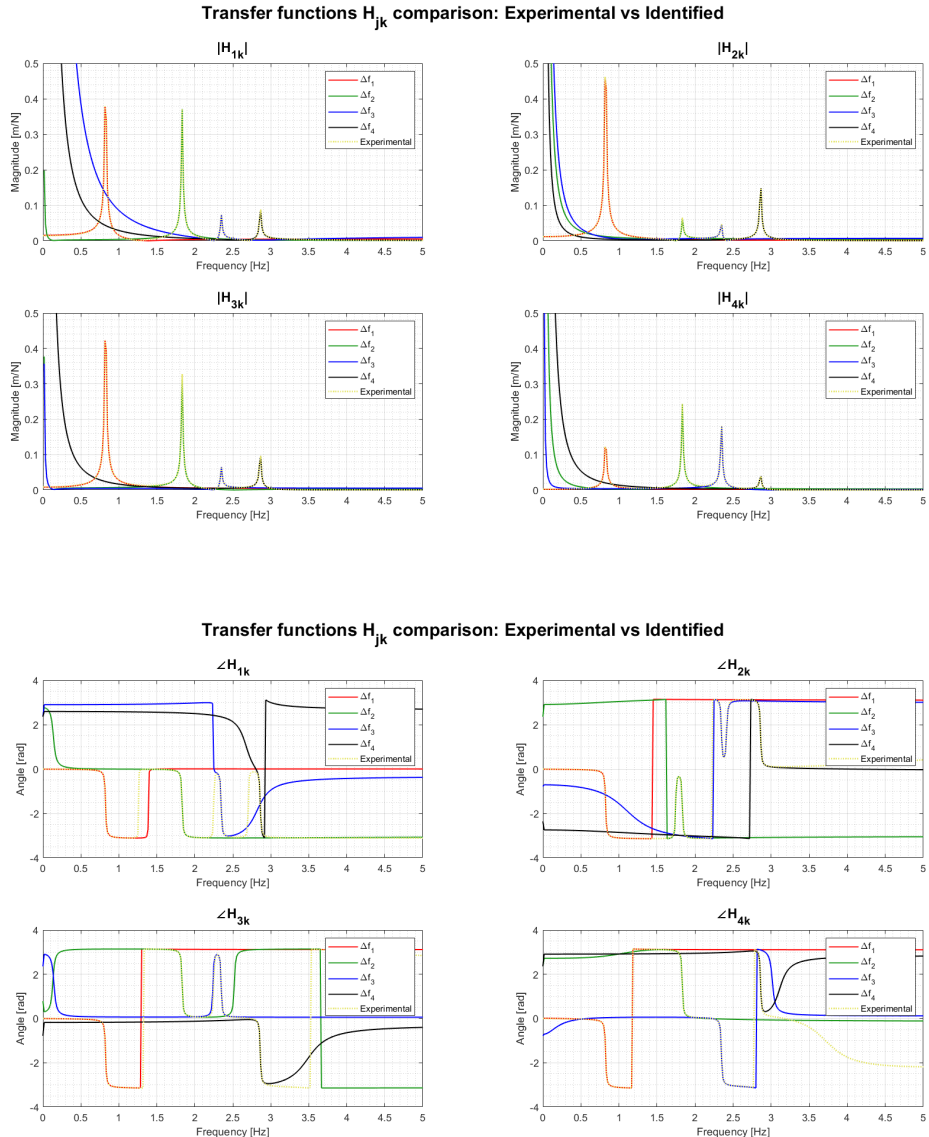


Figure 7: Reconstructed FRFs compared to the experimental one.

## 4 Modal Parameters Comparison

In this section we briefly discuss the differences and similarities between the modal parameters obtained with the minimal residual method and with the simplified one. The values for both methods are reported below:

$$\begin{aligned}
[x_1] &= \begin{bmatrix} 0.0195 & 0.0081 & 0.0064 & 0.0054 \\ 5.1312 & 11.5190 & 14.7652 & 18.0115 \\ 0.2766 & 0.7944 & 0.1885 & 0.2526 \\ 0 & 0 & 0 & 0 \\ 0 & 0 & 0 & 0 \\ 0 & 0 & 0 & 0 \\ 0 & 0 & 0 & 0 \\ 0 & 0 & 0 & 0 \end{bmatrix} \leftrightarrow [x'_1] = \begin{bmatrix} 0.0096 & 0.0043 & 0.0034 & 0.0029 \\ 5.1803 & 11.5155 & 14.7447 & 17.9789 \\ 0.2704 & 0.4258 & 0.1142 & 0.1932 \\ -0.0029 & 0.0053 & 0.0043 & 0.0014 \\ 0.0055 & -0.0004 & 0.0129 & 0 \\ 0.0000 & -0.0001 & -0.0045 & 0 \\ 0 & 0.0008 & 0.9499 & 0.6111 \\ 0 & -0.0020 & -3.8323 & -0.9989 \end{bmatrix} \\
[x_2] &= \begin{bmatrix} 0.0195 & 0.0082 & 0.0066 & 0.0053 \\ 5.1312 & 11.5190 & 14.7652 & 18.0115 \\ 0.3407 & 0.1402 & -0.1307 & -0.4365 \\ 0 & 0 & 0 & 0 \\ 0 & 0 & 0 & 0 \\ 0 & 0 & 0 & 0 \\ 0 & 0 & 0 & 0 \\ 0 & 0 & 0 & 0 \end{bmatrix} \leftrightarrow [x'_2] = \begin{bmatrix} 0.0097 & 0.0043 & 0.0034 & 0.0028 \\ 5.1803 & 11.5155 & 14.7449 & 17.9764 \\ 0.3333 & 0.0746 & -0.0768 & -0.3268 \\ -0.0033 & 0.0009 & -0.0028 & -0.0157 \\ -0.0008 & -0.0042 & -0.0073 & 0 \\ 0.0000 & -0.0005 & 0.0012 & 0 \\ 0 & 0.0544 & -0.2650 & -0.0377 \\ 0 & -0.2302 & 0.3078 & -0.0896 \end{bmatrix} \\
[x_3] &= \begin{bmatrix} 0.0195 & 0.0081 & 0.0064 & 0.0053 \\ 5.1312 & 11.5190 & 14.7652 & 18.0115 \\ 0.3133 & -0.7019 & -0.1673 & 0.2842 \\ 0 & 0 & 0 & 0 \\ 0 & 0 & 0 & 0 \\ 0 & 0 & 0 & 0 \\ 0 & 0 & 0 & 0 \\ 0 & 0 & 0 & 0 \end{bmatrix} \leftrightarrow [x'_3] = \begin{bmatrix} 0.0097 & 0.0044 & 0.0033 & 0.0028 \\ 5.1802 & 11.5155 & 14.7443 & 17.9765 \\ 0.3067 & -0.3795 & -0.0995 & 0.2121 \\ -0.0029 & -0.0037 & -0.0052 & 0.0097 \\ -0.0036 & -0.0032 & 0.0051 & 0 \\ 0.0001 & -0.0000 & 0.0003 & 0 \\ 0 & 0.0012 & 0.0009 & -0.1098 \\ 0 & 0.0040 & -0.0039 & 0.6118 \end{bmatrix} \\
[x_4] &= \begin{bmatrix} 0.0195 & 0.0081 & 0.0064 & 0.0053 \\ 5.1312 & 11.5190 & 14.7652 & 18.0115 \\ 0.0904 & -0.5207 & 0.4745 & -0.1148 \\ 0 & 0 & 0 & 0 \\ 0 & 0 & 0 & 0 \\ 0 & 0 & 0 & 0 \\ 0 & 0 & 0 & 0 \\ 0 & 0 & 0 & 0 \end{bmatrix} \leftrightarrow [x'_4] = \begin{bmatrix} 0.0097 & 0.0044 & 0.0034 & 0.0027 \\ 5.1802 & 11.5158 & 14.7441 & 17.9762 \\ 0.0886 & -0.2839 & 0.2936 & -0.0857 \\ -0.0008 & -0.0017 & 0.0140 & -0.0043 \\ -0.0015 & 0.0027 & 0.0020 & 0 \\ 0.0001 & -0.0004 & 0.0002 & 0 \\ 0 & 0.0368 & -0.0040 & 0.1204 \\ 0 & -0.0823 & 0.0046 & -0.5129 \end{bmatrix}
\end{aligned}$$

We can notice how, with some minor exceptions, even the simplified methods were able to provide a good approximation of the modal parameters. In particular, the natural frequencies are almost equal between the two methods, while the damping ratios and modal constants show bigger differences. These values still remain acceptable since those differences does not translate in changes of the system characteristics and behaviour. The other constants are very close to 0 in both cases. Notice that, in the minimal residual methods, the  $E_j$  and  $F_j$  for the first natural frequency are equal to zero and this reflects the absence of seismographic zone from previous frequencies. The same goes for  $C_j$  and  $D_j$  in correspondence of the fourth natural frequency (absence of quasi-static zone of higher frequencies). In conclusion both methods, in particular the second one, well represent the behaviour of the system. This is further supported by the comparison between the FRFs, which basically show no appreciable difference in a neighborhood of the natural frequencies.

## 5 Modal Approach FRF Reconstruction

First of all we choose the first measurement values for  $m_j$ ,  $c_j$  and  $k_j$ . We chose these arbitrarily since all the values between different measurements are very similar. These values are computed starting from the  $h_j$  and  $\omega_j$  values. From these we can construct the diagonal modal matrices  $M_q$ ,  $C_q$  and  $K_q$ :

$$[M_q] = \begin{bmatrix} 1 & 0 & 0 & 0 \\ 0 & 1 & 0 & 0 \\ 0 & 0 & 1 & 0 \\ 0 & 0 & 0 & 1 \end{bmatrix} \quad (26)$$

$$[C_q] = \begin{bmatrix} 0.0999 & 0 & 0 & 0 \\ 0 & 0.0994 & 0 & 0 \\ 0 & 0 & 0.0999 & 0 \\ 0 & 0 & 0 & 0.0990 \end{bmatrix} \quad (27)$$

$$[K_q] = \begin{bmatrix} 26.854 & 0 & 0 & 0 \\ 0 & 132.6061 & 0 & 0 \\ 0 & 0 & 217.4052 & 0 \\ 0 & 0 & 0 & 323.1655 \end{bmatrix} \quad (28)$$

Having these parameters we can compute the transfer function  $H_q(\Omega)$  using the mechanical impedance matrix  $[D(\Omega)]$ , whose inverse coincides with the frequency response matrix.:

$$H_q(\Omega) = [D_q(\Omega)]^{-1} = [-\Omega^2[M_q] + i\Omega[C_q] + [K_q]]^{-1} \quad (29)$$

The resulting  $H_q(\Omega)$  are reported in figures below:

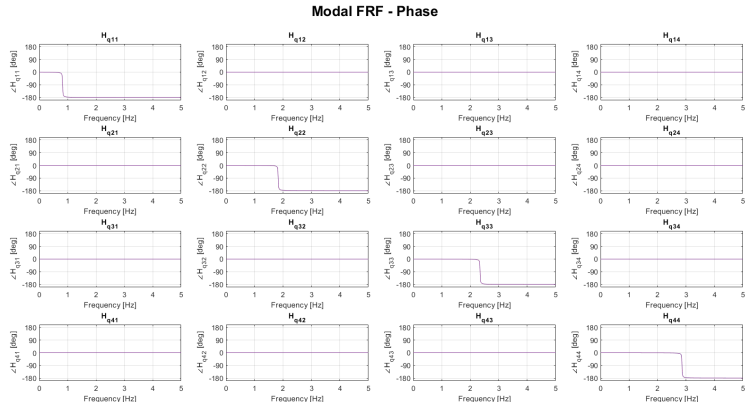
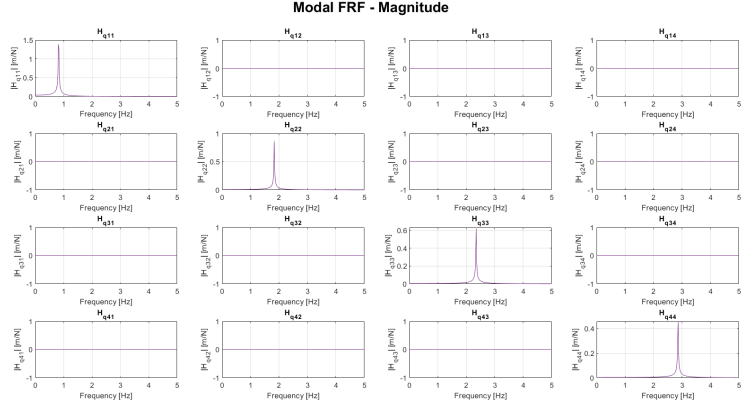


Figure 8: Modal FRF matrix  $H_q$

As expected we get a diagonal matrix in which each magnitude has a single peak in correspondence of its own resonance, where the phase has a  $-\pi$  shift. In order to reconstruct the non-modal FRF we need to compute the following relation, where  $\Lambda_F$  is assumed to be  $[1, 1, 1, 1]$ :

$$[H(\Omega)] = [\Phi][H_q][\Phi]^T \quad (30)$$

In the following graphs we report the  $x_1$ ,  $x_2$ ,  $x_3$  and  $x_4$  FRFs which have been calculated repeating this approach with the modal values obtained from the respective measurement. This choice had only a consistency purpose.

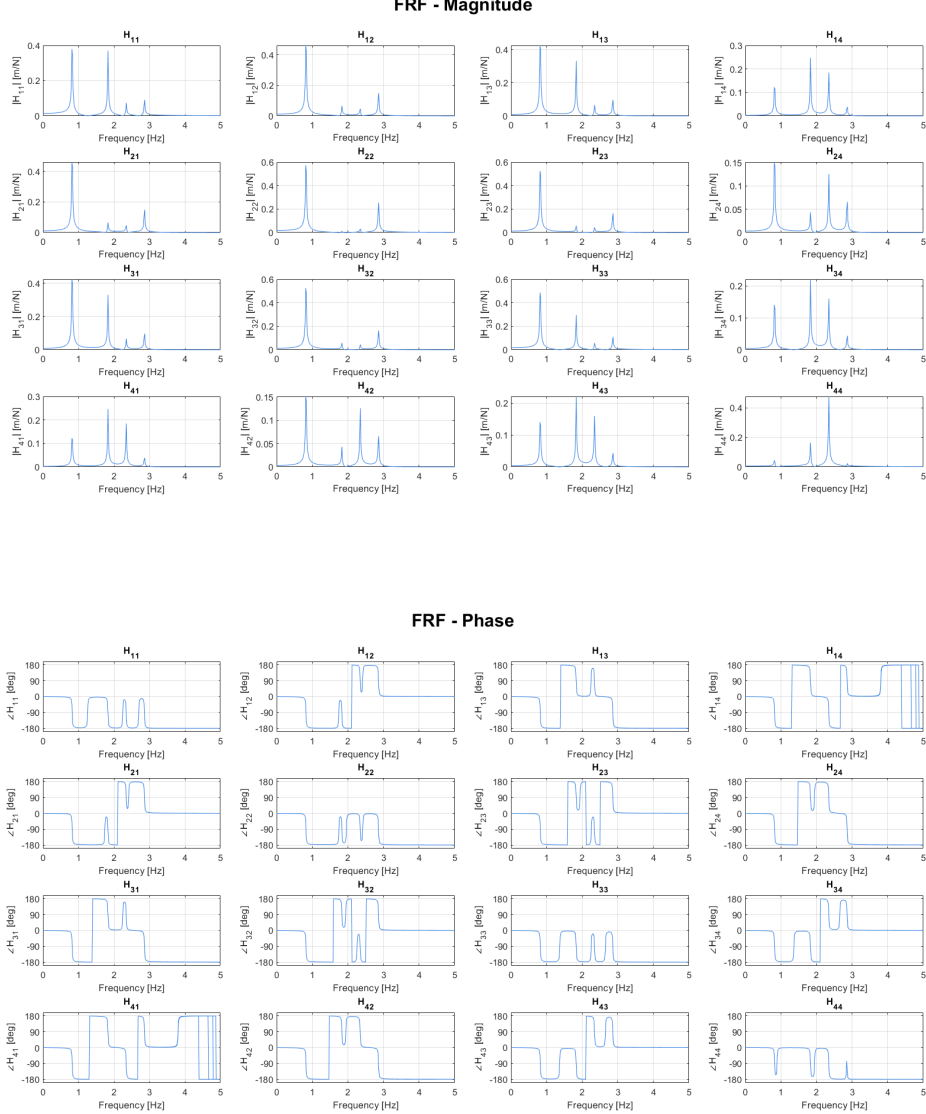


Figure 9: Reconstructed complete FRF matrix

We now plot the FRF matrix compared to the experimental one, considering only the case in which the force is applied in  $x_1$  so we need to introduce  $[\Lambda_F] = [1, 0, 0, 0]$ :

$$[H(\Omega)] = [\Phi][H_q][\Phi]^T[\Lambda_F] \quad (31)$$

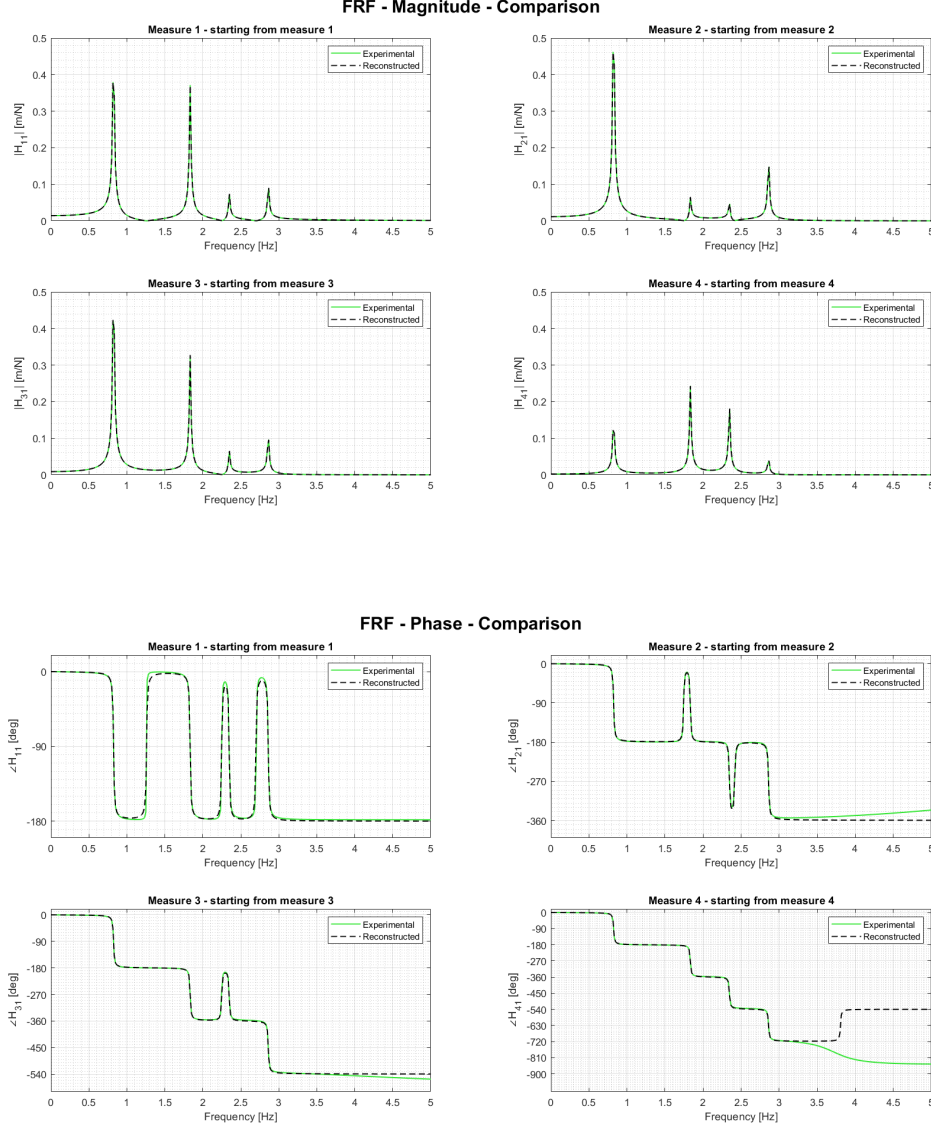


Figure 10: Reconstructed FRF compared to the experimental one.

As we can deduce from the graphs the reconstruction is very accurate except for the phase, which differs from the experimental one for frequencies higher than 3 Hz. This is due to the frequency intervals we chose and the data we had.

## 6 Co-located FRF in $x_2$

In order to evaluate the co-locate FRF in  $x_2$  we select the second row of figure (10) by using the Jacobian  $[\Lambda_F] = [0, 1, 0, 0]$ :

$$[H(\Omega)] = [\Phi][H_q][\Phi]^T[\Lambda_F] \quad (32)$$

In order to evaluate the effect on  $x_2$  only we select the second column of what we just obtained by introducing the same Jacobian  $[\Lambda_F]$  transposed:

$$[H(\Omega)] = [\Lambda_F]^T[\Phi][H_q][\Phi]^T[\Lambda_F] \quad (33)$$

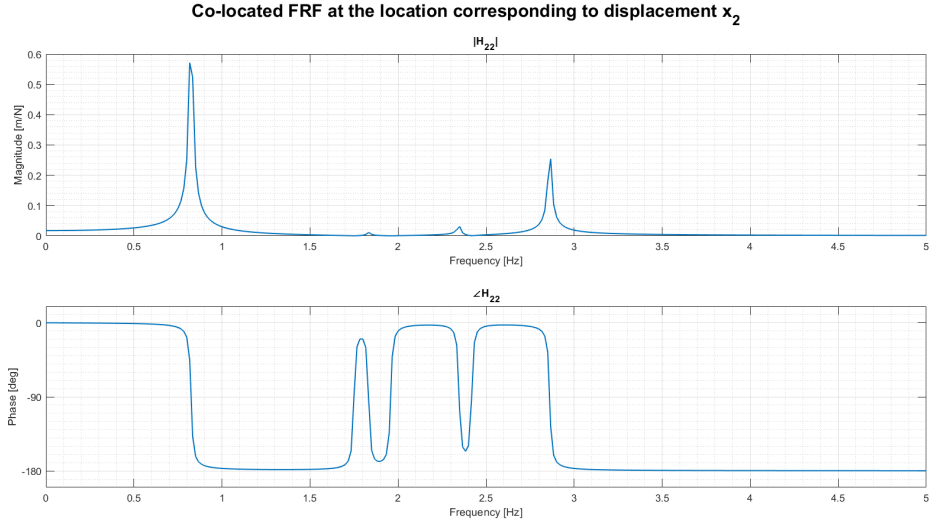


Figure 11: Colocated FRF  $x_2$ .

## 7 System Matrices

We now need to evaluate the generalized  $[M^*]$ ,  $[C^*]$  and  $[K^*]$  system matrices. To do so we rely on the modal matrices  $[M_q]$ ,  $[C_q]$  and  $[K_q]$  and the mode shapes  $[\Phi]$  which are employed in the following relations:

$$[M_q] \approx [\Phi][M^*][\Phi]^T \rightarrow [M^*] = [\Phi]^{-1}[M_q][[\Phi]^T]^{-1} \quad (34)$$

$$[C_q] \approx [\Phi][C^*][\Phi]^T \rightarrow [C^*] = [\Phi]^{-1}[C_q][[\Phi]^T]^{-1} \quad (35)$$

$$[K_q] \approx [\Phi][K^*][\Phi]^T \rightarrow [K^*] = [\Phi]^{-1}[K_q][[\Phi]^T]^{-1} \quad (36)$$

$$[M^*] = \begin{bmatrix} 0.9980 & -0.0034 & -0.0395 & -0.0123 \\ -0.0034 & 0.9731 & -0.0190 & -0.0066 \\ -0.0395 & -0.0190 & 0.9966 & -0.0031 \\ -0.0123 & -0.0066 & -0.0031 & 0.9892 \end{bmatrix} \quad (37)$$

$$[C^*] = \begin{bmatrix} 0.1002 & -0.0015 & -0.0030 & -0.0014 \\ -0.0015 & 0.0992 & -0.0032 & -0.0001 \\ -0.0030 & -0.0032 & 0.1003 & -0.0008 \\ -0.0014 & -0.0001 & -0.0008 & 0.0989 \end{bmatrix} \quad (38)$$

$$[K^*] = \begin{bmatrix} 150.9082 & -97.8385 & -4.1251 & -0.8620 \\ -97.8385 & 196.2740 & -99.3221 & 0.1075 \\ -4.1251 & -99.3221 & 151.1068 & -49.5082 \\ -0.8620 & 0.1075 & -49.5082 & 198.2044 \end{bmatrix} \quad (39)$$

All the matrices are computed using the first data set of  $x_1$  because, as we have observed, the difference between different measurements is negligible.